

1 Using  $^{14}\text{C}$  and  $^3\text{H}$  to understand groundwater flow and recharge in an  
2 aquifer window

3

4 **A.P. Atkinson<sup>1,2</sup>, I. Cartwright<sup>1,2</sup>, B.S. Gilfedder<sup>3</sup>, D. I. Cendón<sup>4,5</sup>, N. P. Unland<sup>1,2</sup>,**  
5 **H. Hofmann<sup>6</sup>**

6 <sup>1</sup>School of Geosciences, Monash University, Clayton, Vic, 3800, Australia.

7 <sup>2</sup>National Centre for Groundwater Research and Training, GPO Box 2100, Flinders University, Adelaide, SA  
8 5001, Australia.

9 <sup>3</sup>Department of Hydrology, University of Bayreuth, Bayreuth, Germany.

10 <sup>4</sup>Australian Nuclear Science and Technology Organisation, Menai, NSW 2232, Australia.

11 <sup>5</sup>School of Biological Earth and Environmental Sciences, The University of New South Wales, Sydney, NSW  
12 2052, Australia.

13 <sup>6</sup>School of Earth Sciences, The University of Queensland, Brisbane, QLD 4072, Australia.

14

15

16

17

18

19

20

21

22

23 Correspondence to: A.P. Atkinson ([alexander.atkinson@monash.edu](mailto:alexander.atkinson@monash.edu))

24

25

26

27

28

29

30

31

## 32 **Abstract**

33 Knowledge of groundwater residence times and recharge locations are vital to the sustainable  
34 management of groundwater resources. Here we investigate groundwater residence times and patterns  
35 of recharge in the Gellibrand Valley, southeast Australia, where outcropping aquifer sediments of the  
36 Eastern View Formation form an ‘aquifer window’ that may receive diffuse recharge from rainfall  
37 and recharge from the Gellibrand River. To determine recharge patterns and groundwater flowpaths,  
38 environmental isotopes ( $^3\text{H}$ ,  $^{14}\text{C}$ ,  $\delta^{13}\text{C}$ ,  $\delta^{18}\text{O}$ ,  $\delta^2\text{H}$ ) are used in conjunction with groundwater  
39 geochemistry and continuous monitoring of groundwater elevation and electrical conductivity. The  
40 water table fluctuates by 0.9 to 3.7 m annually, implying recharge rates of 90 and 372 mm yr<sup>-1</sup>.  
41 However, residence times of shallow (11 to 29 m) groundwater determined by  $^{14}\text{C}$  are between 100  
42 and 10,000 years,  $^3\text{H}$  activities are negligible in most of the groundwater, and groundwater electrical  
43 conductivity remains constant over the period of study. Deeper groundwater with older  $^{14}\text{C}$  ages has  
44 lower  $\delta^{18}\text{O}$  values than younger shallower groundwater, which is consistent with it being derived from  
45 greater altitudes. The combined geochemistry data indicate that local recharge from precipitation  
46 within the valley occurs through the aquifer window, however much of the groundwater in the  
47 Gellibrand Valley predominantly originates from the regional recharge zone, the Barongarook High.  
48 The Gellibrand Valley is a regional discharge zone with upward head gradients that limits local  
49 recharge to the upper 10 m of the aquifer. Additionally, the groundwater head gradients adjacent to  
50 the Gellibrand River are generally upwards, implying that it does not recharge the surrounding  
51 groundwater and has limited bank storage.  $^{14}\text{C}$  ages and Cl concentrations are well correlated and Cl  
52 concentrations may be used to provide a first-order estimate of groundwater residence times.  
53 Progressively lower chloride concentrations from 10,000 years BP to the present day are interpreted to  
54 indicate an increase in recharge rates on the Barongarook High.

55

56

## 57 **1. Introduction**

58 Groundwater residence time can be defined as the period of time elapsed since the infiltration  
59 of a given volume of water (Campana & Simpson, 1984), or perhaps more accurately, the  
60 mean time that a mixture of waters of different ages have resided in an aquifer (Bethke &  
61 Johnson, 2008). The residence time of water within an aquifer is a key parameter in  
62 describing catchment storage and may be used to estimate historical recharge rates (Le Gal  
63 La Salle et al., 2001; Cook et al., 2002; Cartwright & Morgenstern, 2012; Zhai et al., 2013),  
64 elucidate groundwater flowpaths (Gardner et al., 2011; Smerdon et al., 2012), calibrate  
65 hydraulic models (Mazor & Nativ, 1992; Reilly et al., 1994; Post et al., 2013) and  
66 characterize the rate of contaminant spreading (Böhlke and Denver 1995; Tesoriero et  
67 al.,2005). From a water resource perspective, information on groundwater residence times is  
68 required for sustainable aquifer management by identifying the risk posed to groundwater  
69 reserves against over-exploitation (Foster & Chilton, 2003), climate change (Manning et al.,  
70 2012) and contamination (Böhlke, 2002).

71

72 Unconfined aquifers may be recharged over broad regions leading to young groundwater at  
73 shallow depths over broad areas (Cendón et al., 2014). On the other hand, the residence time  
74 of groundwater in confined aquifers generally increases away from discrete recharge areas.  
75 The geology of catchments is often complex and heterogeneous and outcrops of aquifers in  
76 more than one location may provide ‘windows’ for groundwater recharge (Meredith et al.,  
77 2012). It is important to document groundwater flow from such aquifer windows. If they act  
78 as recharge areas, changes in land-use such as agricultural development may introduce  
79 contaminants to the deeper regional groundwater systems. By contrast, if they are local

80 discharge areas, use of regional groundwater from these areas may impact rivers, lake or  
81 wetlands that are receiving groundwater.

82

83 Rivers may also recharge shallow groundwater if the hydraulic gradient between the river and  
84 the groundwater is reversed during high flows (Doble et al., 2012). Episodic recharge of  
85 aquifers by large over-bank floods is also locally important (Moench & Barlow, 2000;  
86 Cendón et al., 2010; Doble et al., 2012), particularly in arid areas (Shentsis & Rosenthal,  
87 2003); however, the potential for over-bank events to recharge aquifers in temperate areas is  
88 still poorly understood. Additionally, during high flow, water from rivers is likely stored  
89 temporarily in the banks (McCallum et al., 2010, Unland et al., 2014); however, the depth  
90 and lateral extent to which bank exchange water infiltrates the aquifer is not well documented.  
91 Lastly, knowledge of residence times of groundwater in close proximity to the river can  
92 provide important information on groundwater-river interactions (Gardner et al., 2011). Local  
93 groundwater flowpaths in connection with rivers are often underlain by deeper regional  
94 flowpaths (Tóth, 1963) however the role these flowpaths play in contributing to river baseflow  
95 remains unclear (Sklash & Farvolden, 1979; McDonnell, 2010; Frisbee & Wilson, 2013;  
96 Goderniaux et al., 2013). This may be elucidated from understanding residence times of near-  
97 river groundwater (Smerdon et al., 2012).

98

99 Radioactive environmental isotopes, in particular  $^{14}\text{C}$  and  $^3\text{H}$  have proven useful tools for  
100 determining groundwater residence times (Vogel, 1974; Wigley, 1975). Produced in the  
101 atmosphere via the interaction of  $\text{N}_2$  with cosmic rays,  $^{14}\text{C}$  has a half life of 5730 years and  
102 can be used to trace groundwater with residence times up to 30 ka. The use of  $^{14}\text{C}$  in dating  
103 groundwater was first discussed by Muennich (1957), and has subsequently been widely used

104 due to the ubiquitous presence of dissolved inorganic carbon (DIC) in groundwater  
105 (Cartwright et al., 2012; Samborska et al., 2012; Stewart, 2012). The calculation of  $^{14}\text{C}$  ages  
106 may be complicated if groundwater DIC is derived from a mixture of sources (Clark and Fritz,  
107 1997). Where a large proportion of DIC is derived from the dissolution of  $^{14}\text{C}$ -free carbonate  
108 minerals in the aquifer matrix, the  $^{14}\text{C}$  originating from the atmosphere or soil zone will be  
109 significantly diluted. Additional sources of  $^{14}\text{C}$  free DIC include old geogenic carbon from  
110 igneous degassing (Bertrand et al., 2013; Frederico et al., 2002) or  $\text{CO}_2$  produced together  
111 with methane from old organic carbon in the aquifer matrix (Aravena et al., 1995).  
112 Groundwaters recharged post 1950 may have anomalously high  $^{14}\text{C}$  activities ( $a^{14}\text{C}$ ) due to  
113 the  $^{14}\text{C}$  produced during atmospheric nuclear tests. Objective  $^{14}\text{C}$  dating requires recognition  
114 and quantification of these processes. A number of models based on both major ion and  
115 stable C isotope geochemistry have been proposed to correct apparent  $^{14}\text{C}$  ages (Han &  
116 Plummer, 2013)

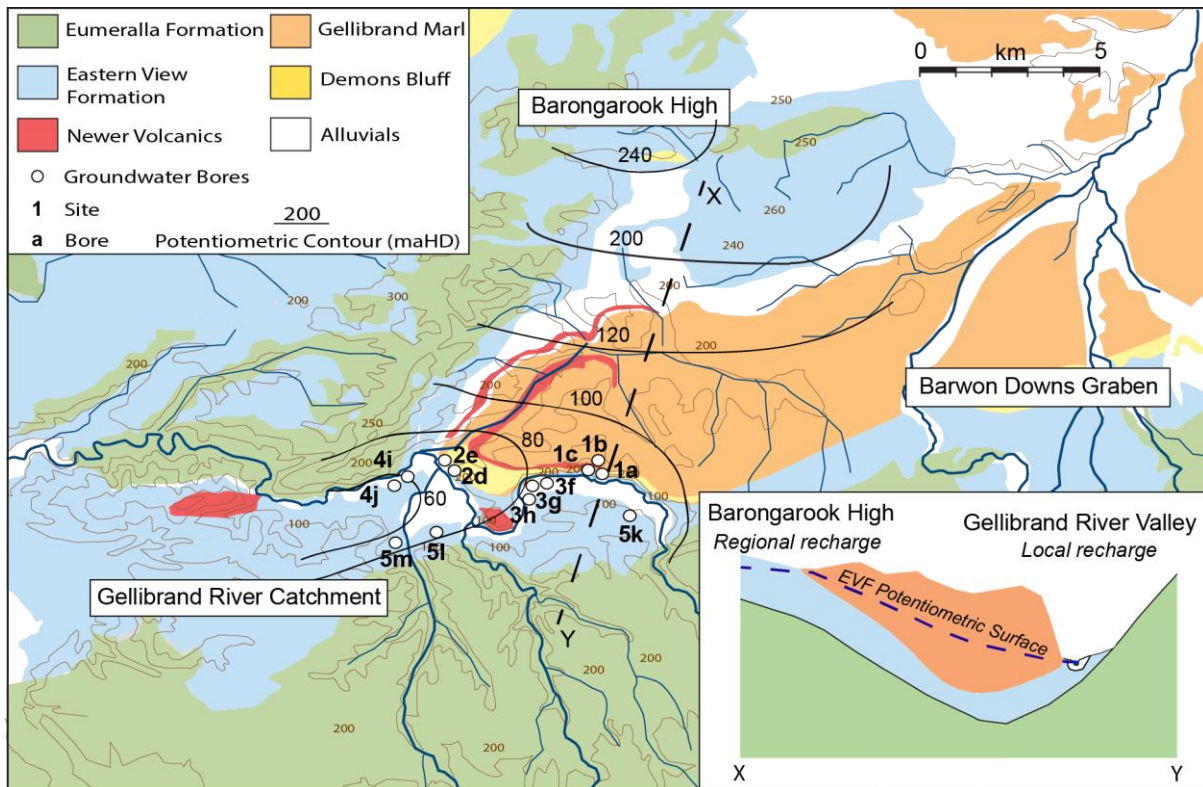
117

118 With a significantly shorter half-life (12.33 years),  $^3\text{H}$  can be used to date groundwater with  
119 residence times of up to 100 years (Vogel et al., 1974). With the decay of the 1960s  $^3\text{H}$  bomb-  
120 pulse peak in the southern hemisphere to near background levels unique ages may now be  
121 determined from single  $^3\text{H}$  measurements (Morgenstern et al., 2010). As  $^3\text{H}$  is part of the  
122 water molecule, there is negligible change to  $^3\text{H}$  activities other than decay, and  $^3\text{H}$  is an  
123 excellent tracer for the movement of water through hydrological systems (Michel, 2004).  
124 Used in conjunction with  $^{14}\text{C}$  data,  $^3\text{H}$  may also be used to study mixing in shallow aquifers  
125 (Le Gal La Salle 2001; Cartwright & Morgenstern, 2012).

126

127

128 **2. Study Site**



129  
 130 **Figure 1** – Geology, groundwater flow, and cross sectional view of the upper part of the Gellibrand  
 131 River Catchment (the Gellibrand Valley). Potentiometric contours for the Eastern View Formation are  
 132 created from groundwater data (Water Resources Data Warehouse, 2013) and are expressed in metres  
 133 above Australian Height Datum (mAHD). Sampled groundwater bores are also shown. Letters refer to  
 134 bores in Table 1.

135

136

137 The Otway Basin is located in southwest Victoria, covering an area of 150,000 km<sup>2</sup>. The  
 138 basin was formed during the Cretaceous rifting of Australia and Antarctica (Briguglio et al.,  
 139 2013) and is infilled with Upper Cretaceous and Cenozoic siliciclastic and calcareous  
 140 sediments that form several aquifers and aquitards. The basin is divided into a number of sub-  
 141 basins with regional groundwater flow paths originating at topographic highs. The Gellibrand  
 142 River Catchment is one of these sub-basins. This study focuses on a 250 km<sup>2</sup> upland area of

143 the Gellibrand River Catchment (known as the Gellibrand Valley), which lies at the foothills  
144 of the Otway Ranges, directly south of the Barongarook High (Fig.1).

145

146 Cretaceous Otway Group sediments of the Eumeralla Formation form the basement of the  
147 catchment and crop out in areas of higher relief. The Eumeralla Formation consists of thickly  
148 bedded siltstone, mudstone and volcanolithic sandstone. It has a low primary porosity and  
149 hydraulic conductivity and acts as a poor aquifer (Lakey & Leonard, 1982). Cenozoic  
150 sediments of the Wangerrip group overlie the bedrock and form major aquifers in the region  
151 to which flow is constrained (Van den Berg, 2009). The primary aquifer in the study area is  
152 the Eastern View Formation or the equivalent Dilwyn Formation (Van den Berg 2009;  
153 Petrides & Cartwright 2006; Atkinson et al., 2013) that is composed of gravel, fine to coarse  
154 grained sand, and major clay layers. The Eastern View Formation comprises predominantly  
155 quartz, feldspars and carbonates (< 2 %) and has hydraulic conductivities of  $10^{-2}$  to  $10^2$  m d<sup>-1</sup>  
156 (Hortle et al., 2011). The Eastern View Formation is underlain by another productive aquifer,  
157 the Pebble Point Formation, however this is much thinner and is separated from the above  
158 layers by the Pember Mudstone. To the north, the Eastern View Formation is confined by the  
159 Gellibrand Marl, which is a regional aquitard that comprises 100 to 200 m of clay, and the  
160 Demons Bluff formation, which comprises fine-grained silts. Basaltic intrusions of the  
161 Quaternary Newer Volcanics are also present. The floodplain is covered with recent alluvial  
162 deposits of sand and clay. Regional groundwater recharge occurs on the Barongarook High  
163 where the Eastern View Formation crops out. Groundwater flows southwest along the  
164 Gellibrand River Catchment from the Barongarook High as well as eastward into the Barwon  
165 Downs Graben. However there is also potential for localised recharge within the Gellibrand  
166 Valley, where outcropping sediments of the Eastern View Formation, potentially act as an  
167 aquifer window (Fig. 1).

168 The Gellibrand Valley contains a mixture of cool temperate rainforest on the valley sides and  
169 cleared agricultural pasture through which the Gellibrand River flows. Rainfall across the  
170 catchment averages  $\sim 1000 \text{ mm yr}^{-1}$ , with the majority of rainfall falling in the Australian  
171 winter between June and September (Bureau of Meteorology, 2013). The Gellibrand River is  
172 gaining and groundwater contributes between 10 and 50% to total river flow dependent on  
173 flow conditions (Atkinson et al., 2013). River flows are between  $5 \times 10^4 \text{ m}^3 \text{ day}^{-1}$  and  $2 \times 10^6$   
174  $\text{m}^3 \text{ day}^{-1}$  (Fig. 2c), with low flows during summer months (December to March) and high  
175 flows and flooding during winter (June to August) (Victorian Water Resources Data  
176 Warehouse, 2013). During flooding there is the potential for aquifer recharge from overbank  
177 flow.

178

179 Although groundwater residence times in the Otway Basin have been explored in the  
180 Gambier Embayment (Love et al., 1994) and nearby Barwon River Graben (Petrides &  
181 Cartwright, 2006), little is known of the residence times of groundwater in the Gellibrand  
182 River Catchment. This is despite the groundwater in Eastern View Formation being a  
183 potential valuable water resource (Petrides & Cartwright, 2006). Here we evaluate  
184 groundwater residence times in the Gellibrand Valley where the Eastern View Formation is  
185 exposed, forming an aquifer window, and regular episodic river floods occur, to understand  
186 the origins of groundwater within the valley and to identify whether groundwater recharge  
187 via rainfall and/or the river occurs in this part of the groundwater system. This is important in  
188 understanding the potential impacts of landuse change and pollution in the catchment as well  
189 as understanding the dynamics of recharge in catchments where aquifer material is exposed  
190 in more than one location. It is also important to fully understand groundwater systems such  
191 as this that have the potential to be developed as significant water resources. Radioactive  
192 tracers  $^{14}\text{C}$  and  $^3\text{H}$  are used to determine residence times and define groundwater flow paths



193 whilst major ion chemistry is employed to determine dominant geochemical processes. Water  
194 table fluctuations and groundwater electrical conductivities are also continuously monitored.  
195 These easily measurable, robust parameters can be used to observe changes in storage and  
196 infer sources of aquifer recharge (Vogt et al., 2010) and allow for comparison with  
197 radioisotopes in understanding the dynamics of groundwater systems. Together, isotopic and  
198 physico-chemical approaches provide insight on both short-term recharge processes (electrical  
199 conductivity, water levels) and long-term recharge processes ( $^3\text{H}$  and  $^{14}\text{C}$ ).

200

### 201 **3. Methods**

202 A number of groundwater monitoring bores that form part of the Victorian State Observation  
203 Bore network are present in the Gellibrand Valley (Victorian Water Resources Data  
204 Warehouse, 2013). These are screened in the Eastern View Formation, with depths of  
205 between 0 and 42 m. Bores located within 25 m from the Gellibrand River generally have  
206 screen depths between 11 and 15 m, whilst bores located on the flood plain have depths  
207 between 21 and 42 m. Groundwater from the Eastern View Formation was sampled from 13  
208 bores. 10 of these are located within 25 m from the river in a 14 km<sup>2</sup> area of the catchment  
209 (Sites 1 to 4 in Fig. 1), with 3 further samples taken from bores situated further back on the  
210 flood plain between 1 and 2 km from the river (Site 5 in Fig. 1). Groundwater was sampled  
211 using an impeller pump set in the screen, with 2 to 3 bore volumes purged before sampling.  
212 Groundwater samples were collected in 1L, 0.25L and 0.125L HDPE bottles and stored at  
213  $\sim 4^\circ\text{C}$  until analysis. In the field, samples for anion analysis were filtered through 0.45 $\mu\text{m}$   
214 cellulose nitrate filters, whilst samples for cation analysis were filtered and acidified with  
215 high purity 16 N  $\text{HNO}_3$  to  $\text{pH} < 2$ . Additionally, electrical conductivity (EC) and pH of  
216 groundwater were measured in the field using a calibrated TPS WP-81 conductivity/pH meter

217 and probes. To assess transient changes in groundwater levels and EC, Aqua Troll 200 (In-  
218 Situ) data loggers were deployed in June 2011. A significant drop in EC in near-river  
219 groundwater is shown in some bores following flooding in June 2012 when bores were  
220 overtopped. However immediately upon pumping in October 2012 (bores 3g, 4i) and April  
221 2013 (bore 1b), the EC of the groundwater returned to pre-flood EC values. We interpret this  
222 as floodwater that infiltrated down the bore which was not displaced by groundwater prior to  
223 pumping, and these data have been omitted. Rainfall samples were also collected in the  
224 catchment throughout the study period for chemical analysis.

225

226 Cations were analysed on filtered, acidified samples using a Thermo Finnigan X Series II  
227 Quadrupole ICP-MS. Anions were measured on filtered unacidified samples using a  
228 Metrohm ion chromatograph. The precision of major ion concentrations based on replicate  
229 analyses is  $\pm 2$  %. Charge balances are within  $\pm 5$  %. Stable isotope ratios were measured  
230 using Finnigan MAT 252 and ThermoFinnigan DeltaPlus Advantage mass spectrometers.  
231  $\delta^{18}\text{O}$  values were measured via equilibration with He- $\text{CO}_2$  at  $32^\circ\text{C}$  for 24 to 48hr in a  
232 Finnigan MAT Gas Bench whilst  $\delta^2\text{H}$  values were measured by the reaction of water samples  
233 with Cr at  $850^\circ\text{C}$  using a Finnigan MAT H/Device. Both  $\delta^{18}\text{O}$  and  $\delta^2\text{H}$  were measured against  
234 an internal standard that has been calibrated using the IAEA, SMOW, GISP and SLAP  
235 standards. Data was normalised following methods outlined by Coplen (1988) and are  
236 expressed relative to V-SMOW where  $\delta^{18}\text{O}$  and  $\delta^2\text{H}$  values of SLAP are  $-55.5\text{‰}$  and  $-428\text{‰}$   
237 respectively. Precision is  $\pm 1\text{‰}$  for  $\delta^2\text{H}$  and  $\pm 0.2\text{‰}$  for  $\delta^{18}\text{O}$ .

238

239  $^{14}\text{C}$  and  $^3\text{H}$  samples of groundwater were measured at the Australian Nuclear Science and  
240 Technology Organisation (ANSTO) and the Tritium and Water Dating Laboratory, Institute

241 of Geological and Nuclear Sciences (GNS), (New Zealand). For  $^{14}\text{C}$  analysis performed at  
242 ANSTO,  $\text{CO}_2$  was extracted from water samples in a vacuum line using orthophosphoric acid  
243 and converted to graphite through reduction with excess  $\text{H}_2$  gas in the presence of an iron  
244 catalyst at  $600^\circ\text{C}$ .  $^{14}\text{C}$  concentrations were measured using a 10kV tandem accelerator mass  
245 spectrometer.  $\delta^{13}\text{C}$  values for these samples are derived from the graphite fraction used for  
246 radiocarbon via EA-IRMS.

247

248 For  $^{14}\text{C}$  samples measured at GNS,  $\text{CO}_2$  was extracted from groundwater samples through  
249 addition of orthophosphoric acid.  $\text{CO}_2$  was made into a graphite target and analysed by AMS.  
250 An aliquot of the extracted  $\text{CO}_2$  was used for  $\delta^{13}\text{C}$  analysis.  $^{14}\text{C}$  activities are expressed as  
251 pMC (percent modern carbon) where pMC = 100% corresponds to 95% of the  $^{14}\text{C}$   
252 concentration of NBS oxalic acid standard (Stuiver and Polach, 1977), with a precision of  
253  $^{14}\text{C}/^{12}\text{C}$  ratios of  $\pm 0.5$  (Fink et al 2004). At both ANSTO and GNS, samples for  $^3\text{H}$  were  
254 distilled and electrolytically enriched prior to being analysed by liquid scintillation counting  
255 as described by Neklapilova et al. (2008a,b) and Morgenstern and Taylor (2009).  $^3\text{H}$  activities  
256 are expressed in Tritium Units (TU) with a relative uncertainty of  $\pm 5\%$  and a quantification  
257 limit of 0.13 to 0.14 TU at ANSTO and 0.02 TU and a relative uncertainty of  $2\%$  at GNS.

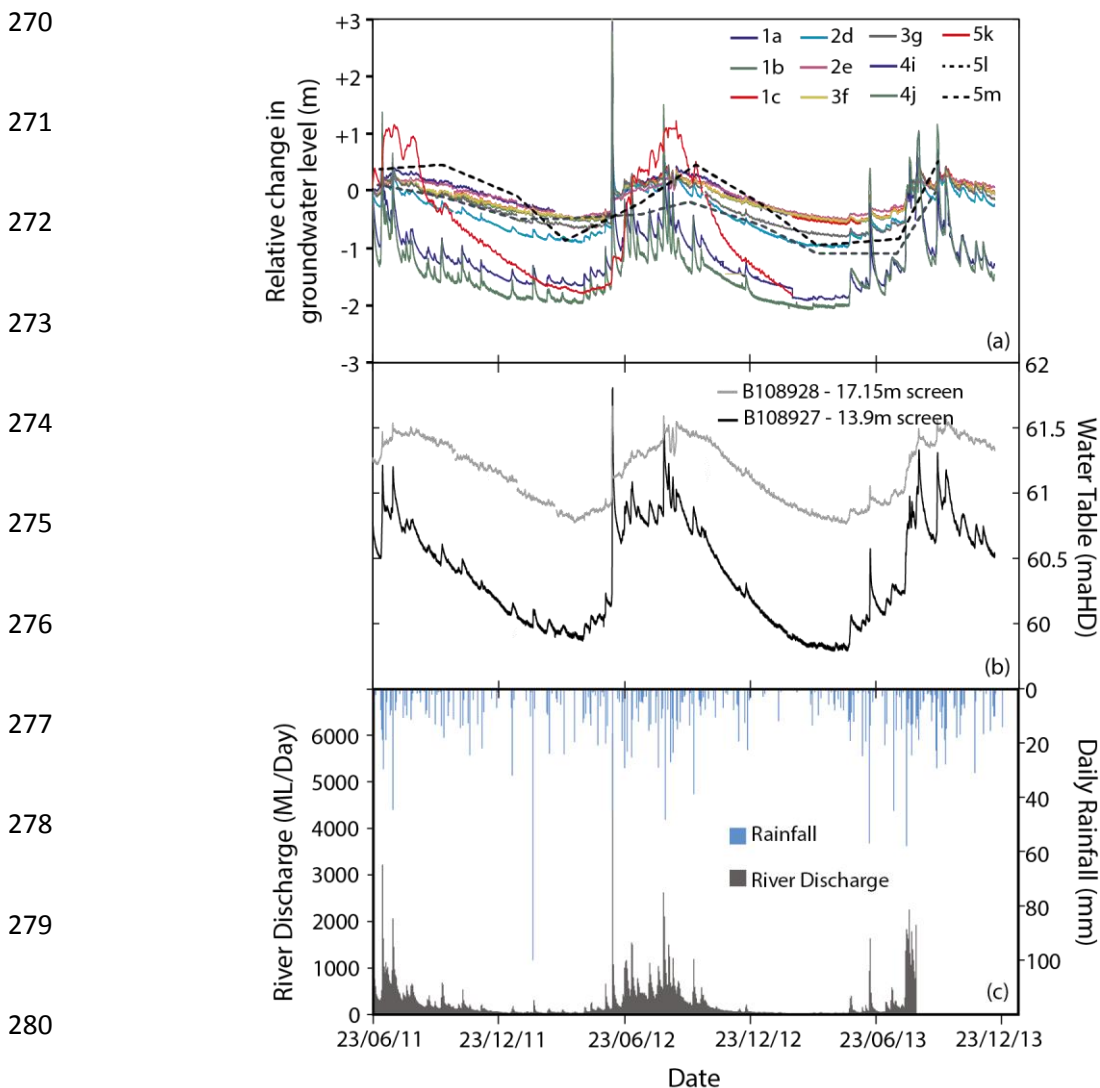
258

## 259 **(4) Results**

### 260 *(4.1) Groundwater elevations*

261 Groundwater elevations decrease from 230 m relative to the Australian Height Datum (AHD)  
262 on the Barongarook High to  $<60$  mAHD within the Gellibrand Valley (Fig.1), with  
263 groundwater flowing from the Barongarook High towards the Gellibrand Valley and then

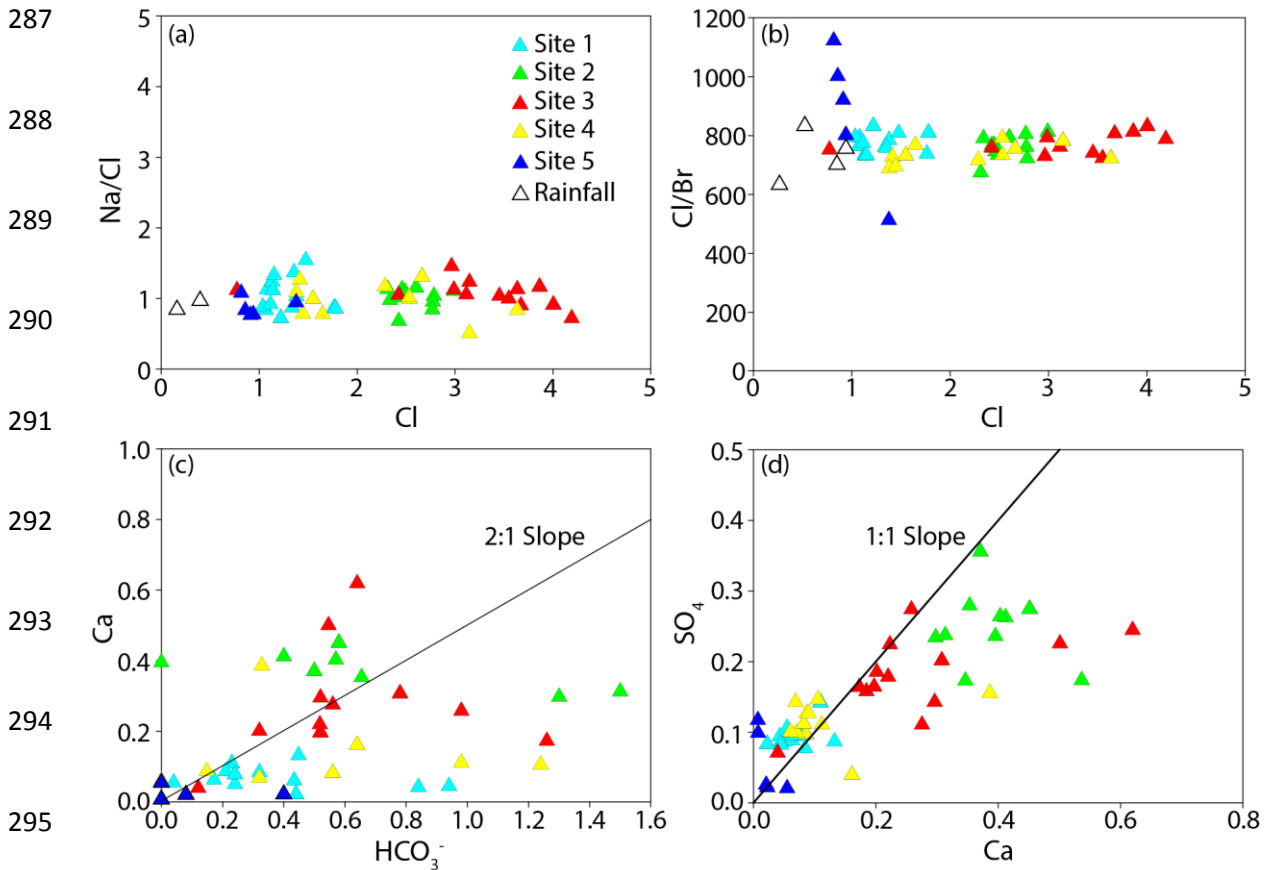
264 westward. Groundwater elevations from all depths and positions within the Gellibrand Valley  
 265 are in phase and fluctuate between 1 and 3 m annually (Fig. 2a). The water table rises  
 266 between June and August following winter rainfall (Fig. 2c) and head gradients at nested sites  
 267 are upwards (Fig. 2b). The Gellibrand River has high water levels that result in flooding  
 268 during winter months (June to August) and low flows in summer (December to March) (Fig.  
 269 2c).



281  
 282 **Figure 2** - (a) Groundwater elevations in bores display clear annual cycles (b) Groundwater head-  
 283 gradients in the Gellibrand Valley are upwards implying a discharge zone (Victorian Water Resources

284 Data Warehouse, 2013) (c) Flow in the Gellibrand River. Baseflow conditions during summer months  
 285 transition into high flows in winter following winter rainfall. (Bureau of Meterology, 2013)

286 (4.2) Groundwater Geochemistry



296  
 297 **Figure 3** – Geochemical characteristics of groundwater in the Eastern View Formation; (a) mCl/Br v  
 298 mCl (b) mNa/Cl v mCl (c) mCa v mHCO<sub>3</sub><sup>-</sup> (d) mSO<sub>4</sub> v mCa. Rainfall samples are also plotted where  
 299 measured. Data is from Table 1 with repeat measurements over the sampling period included.

300  
 301 The chemistry of groundwater in the Gellibrand Valley is summarised in Table 1.  
 302 Groundwater is oxic, with electrical conductivities between 140 and 600  $\mu\text{S cm}^{-1}$  and pH  
 303 values ranging from 4.8 to 6.0. Groundwater from close proximity to the river (Sites 1 to 4)  
 304 generally has higher EC values (144 to 545  $\mu\text{S cm}^{-1}$ ) than groundwater further back on the  
 305 floodplain at site 5 (149 to 220  $\mu\text{S cm}^{-1}$ ). Despite the range of salinity, the relative

306 proportions of the major ions in groundwater are similar across the catchment. The  
307 groundwater is Na-Cl type. Cl constitutes between 68 and 92% of total anions on a molar  
308 basis, with  $\text{HCO}_3$  accounting for 0 to 25%. Increases in Cl concentrations are associated with  
309 a decrease in  $\text{HCO}_3$ . Na comprises between 60 and 85% of total cations with Ca constituting  
310 1 to 10%, Mg constituting 0 to 10% and K constituting 0 to 10%. Increased Na  
311 concentrations are associated with decreases in both Ca and Mg concentrations. Molar Cl/Br  
312 ratios are between 400 and 600 and do not increase with increasing Cl (Fig. 3b), molar Na/Cl  
313 ratios are 0.7 to 1.3 and also remain stable with increasing Cl concentrations (Fig. 3a). Na/Cl  
314 ratios of groundwater samples are similar to those measured in rainfall in southeast Australia  
315 (Blackburn and Mcleod, 1983) and the Cl/Br ratios are also similar to those expected for local  
316 rainfall (Cartwright et al., 2006). There is a weak correlation between Ca and  $\text{HCO}_3$  (Fig. 3c)  
317 and between Ca and  $\text{SO}_4$  (Fig. 3d).

318

#### 319 (4.3) $^{13}\text{C}$ , $\delta^{14}\text{C}$ and $^3\text{H}$ concentrations

320 The  $\delta^{14}\text{C}$  of groundwater ranges from 29 to 101.5 pMC.  $^3\text{H}$  activities are below detection for  
321 the majority of groundwater samples (Table 1), with the exception of bores 5k, 5l and 5m  
322 which have activities of 1.02, 1.47 and 1.24 TU, respectively. Groundwater from these bores  
323 has  $\delta^{14}\text{C} > 90$  pMC. The distribution of  $\delta^{14}\text{C}$  and  $^3\text{H}$  values across the catchment is  
324 heterogeneous with no relationship to depth or along lateral groundwater flowpaths. A strong  
325 inverse correlation ( $R^2 = 0.87$ ) is observed between  $\delta^{14}\text{C}$  and Cl concentrations (Table 1). A  
326 similar correlation is also observed for Na ( $R^2 = 0.855$ ), K ( $R^2 = 0.82$ ), Ca ( $R^2 = 0.6$ ) and Mg  
327 ( $R^2 = 0.54$ ).

328

329

330

331 (4.4) Stable Isotopes ( $\delta^2\text{H}$ ,  $\delta^{18}\text{O}$ ,  $\delta^{13}\text{C}$ )

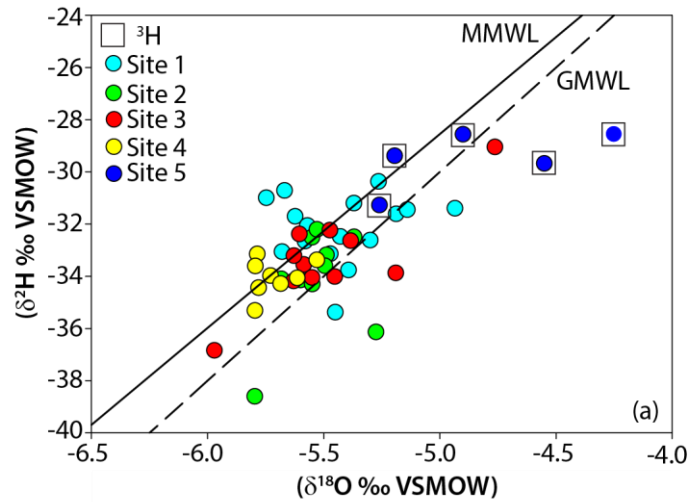
332

333

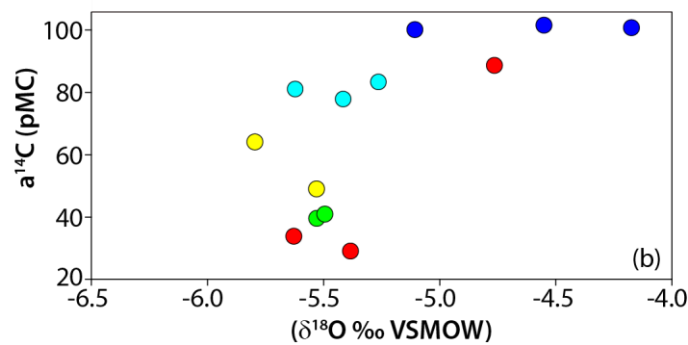
334

335

336



337



340

341 **Figure 4** – (a)  $^2\text{H}$  vs  $^{18}\text{O}$  values of the Gellibrand River and surrounding groundwater sampled over  
342 March 2011 – August 2013 and the weighted average for rainfall from Adelaide and Melbourne.  
343 MMWL = Melbourne Meteoric Water Line (Hughes and Crawford, 2012). GMWL = Global Meteoric  
344 Water Line (Clarke and Fritz, 1997). Groundwaters with  $^3\text{H}$  activities  $> 1$  TU are also highlighted.  
345 Data is from Table 1 with repeat measurements over the sampling period included. (b)  $a^{14}\text{C}$  vs  $^{18}\text{O}$  of  
346 groundwater samples.

347

348  $\delta^{18}\text{O}$  and  $\delta^2\text{H}$  values of groundwater define a narrow field ( $\delta^{18}\text{O} = -4$  to  $-6$  ‰ and  $\delta^2\text{H} = -28$   
349 to  $-40$  ‰) that is close to both the global and local meteoric water lines (Fig. 4a). The  
350 Gellibrand Valley is located between Melbourne and Adelaide, with groundwater generally  
351 plotting between the average isotopic compositions of meteoric waters located in those areas.

352 Groundwater samples from site 5 are enriched in both  $\delta^{18}\text{O}$  (+ 0.7 ‰) and  $\delta^2\text{H}$  (+ 3.5 ‰)  
353 relative to groundwater from sites 1 to 4 and have  $^3\text{H}$  activities >1 TU (Fig. 4a). Additionally  
354 samples that are enriched in  $\delta^{18}\text{O}$  have a  $^{14}\text{C}$  >100 pMC (Fig. 4b).  $\delta^{13}\text{C}$  values of DIC from  
355 groundwater range from -19.8 to -25 ‰, with an average of 21.7‰ (Table 1)

356

#### 357 (4.5) Continuous Electrical Conductivity

358 Continuous groundwater EC records for a number of near-river bores and 5k, which is  
359 situated on the flood-plain, are shown in conjunction with changes in river height for the  
360 study period (Fig. 5). Groundwater EC in all bores for the majority of the dataset show little  
361 or no response to changes in river height, although minor dilution of groundwater EC occurs  
362 during high flow events in August and September 2013. Minor changes in EC correlate to  
363 sampling events in which groundwater bores were pumped

364

365

366

367

368

369

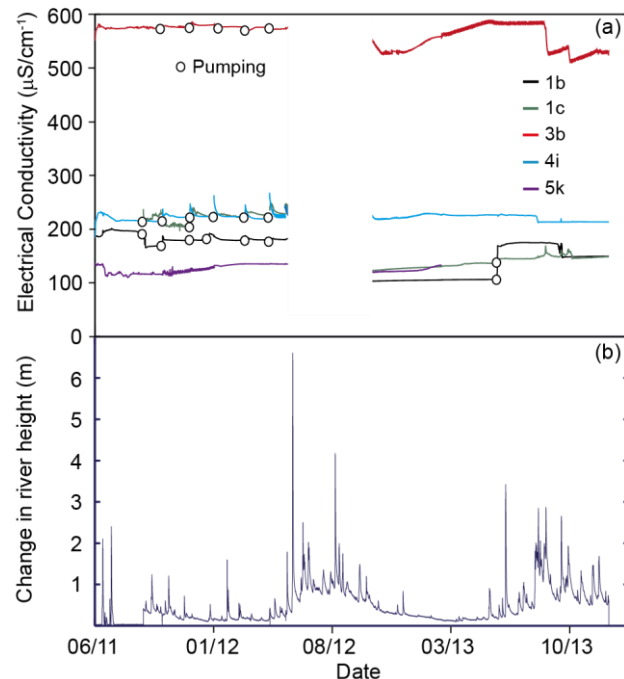
370

371

372

373

374





375 **Figure 5** – (a) Continuous electrical conductivity monitoring of near-river groundwater. (b). Changes  
376 in river height over the study period. Groundwater EC and river level data from deployed Aqua troll  
377 200 (In-Situ) Data Loggers.

378

## 379 **(5) Discussion**

380

### 381 *(5.1) Groundwater Chemistry*

382 Understanding geochemical processes in groundwater is required for correction of  $^{14}\text{C}$  ages  
383 and in documenting groundwater flow and recharge. Processes which govern the evolution of  
384 groundwater geochemistry and sources of solutes in the Eastern View Formation can be  
385 determined from the major ion geochemistry. The observation that Cl/Br ratios are between  
386 500 and 1000, which is similar to those expected in rainfall, and do not increase with  
387 increased TDS implies that evapotranspiration rather than halite dissolution is the major  
388 process controlling groundwater salinity (Herczeg et al., 2001; Cartwright et al., 2006). This  
389 conclusion is also consistent with an absence of halite in the aquifer lithologies. The  $\delta^{18}\text{O}$  and  
390  $\delta^2\text{H}$  values of groundwater generally lie close to the meteoric water line and do not define  
391 evaporation trends, implying that transpiration in the soil zone or upper parts of the aquifer is  
392 likely to be more dominant over evaporation. Na/Cl ratios in groundwater are also similar to  
393 those in local rainfall ( $\sim 1$ ) implying that silicate weathering is limited (e.g., Edmunds et al.,  
394 2002), whilst the increase in Na concentrations at the expense of Ca may indicate ion  
395 exchange reactions on the surface of clay minerals (e.g., Herczeg et al., 2001). That Ca and  
396  $\text{mHCO}_3$  are poorly correlated suggests that negligible dissolution of calcite has occurred. A  
397 handful of groundwater samples have a 1:1 Ca: $\text{SO}_4$  ratio indicating some minor gypsum  
398 dissolution may take place. Together, the major ion geochemistry suggests that water-rock  
399 interaction is limited with minimal silicate weathering, negligible dissolution of halite and  
400 carbonate minerals and some minor dissolution of gypsum. As is the case elsewhere in

401 southeast Australia, including within the Otway basin, the primary geochemical process is  
402 evapotranspiration promoted by the moderate rainfall and water-efficient native vegetation,  
403 and the groundwater salinity is largely controlled by the degree of evapotranspiration during  
404 recharge (Herczeg et al., 2001; Bennetts et al., 2006; Petrides & Cartwright, 2006).

405

406 Groundwater from the near-river sites 1 to 4 has lower  $\delta^{18}\text{O}$  and  $\delta^2\text{H}$  values relative to that  
407 from the floodplain away from the river at site 5. In a catchment of  $< 250 \text{ km}^2$  with a  $^{14}\text{C}$   
408 varying between 29.1 to 101.5 pMC, climatic influences and the altitude effect are the most  
409 likely drivers in variability between groundwater samples (e.g., Dansgaard, 1964). As there is  
410 potential for groundwater recharge on the elevated Barongarook High and within the  
411 Gellibrand Valley; the depleted stable isotope signature of groundwater at sites 1 to 4 relative  
412 to groundwater samples from site 5 may reflect altitudinal differences of groundwater  
413 recharged at these locations. Assuming typical altitudinal gradients in rainfall of  $-0.15\text{‰}$  to  $-$   
414  $0.5\text{‰}$  per 100 m for  $\delta^{18}\text{O}$  (Clark & Fritz, 1997) and an elevation difference of  $\sim 150\text{m}$   
415 between the Gellibrand Valley and the Barongarook High, groundwater recharged on the  
416 Barongarook High is expected to be depleted in  $^{18}\text{O}$  by  $-0.25\text{‰}$  to  $-0.75\text{‰}$  relative to that  
417 which is locally recharged in the valley.  $\delta^{18}\text{O}$  values of groundwater from sites 1 to 4 are  
418  $\sim -0.7\text{‰}$  lower than groundwater from site 5. Thus, the stable isotopes indicate that water in  
419 the near-river environment may have been recharged from the Barongarook High, whilst  
420 water from the floodplain is recharged locally within the valley. This is supported by the  
421 negligible  $^3\text{H}$  activities at sites 1 to 4, which indicate old water, and elevated activities at site  
422 5 indicating recently recharged water. It is possible that the differences in stable isotopes  
423 between the sites are driven by climatic factors rather than altitude.

424

425 It is also possible that the variations in  $\delta^{18}\text{O}$  values represent variation in the climate during  
426 recharge. While this has been proposed elsewhere in the Otway Basin (Love et al., 1994), in  
427 this part of the Otway Basin climatic variation has not been recorded in groundwater  $\delta^{18}\text{O}$   
428 values (Petrides and Cartwright, 2006). The lack of a systematic variation in  $\delta^{18}\text{O}$  values with  
429  $\text{a}^{14}\text{C}$  in groundwater from sites 1 to 4 also indicates that a climatic influence on  $\delta^{18}\text{O}$  values is  
430 unlikely.

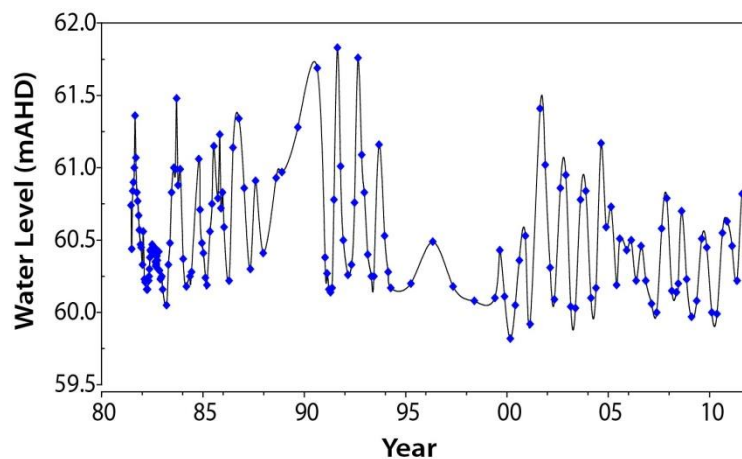
431

### 432 (5.2) Water Table Fluctuations

433 Annual cycles of groundwater elevations are present in all groundwater bores, which are  
434 screened 11 to 40 m below the ground surface. The fluctuations in groundwater levels across  
435 the Gellibrand Valley are likely a pressure response to recharge on the flood plain following  
436 rainfall events via hydraulic loading (Cartwright et al., 2007; Brodie et al., 2008; Unland et  
437 al., 2014). The magnitude of annual water table fluctuations recorded in data loggers is  
438 similar to those over the previous 30 years (Fig.6).

439

440



444

445 **Figure 6** – Historical water table fluctuations 1988-2011 for bore 108927 (Victorian Water Resources  
446 Data Warehouse, 2013). The magnitude of annual recharge cycles are coherent with those recorded in  
447 data loggers over the study period (2011 to 2013)

448

449

450 Recharge was estimated for years 2012 and 2013 using the water-table fluctuation method

451 Eq.(1):

$$452 \quad R = S_y * \Delta h / \Delta t \quad (1)$$

453 (Scanlon et al., 2002), where  $S_y$  is specific yield,  $\Delta h$  is the change in water table height

454 between the hydrograph recession and hydrograph peak and  $\Delta t$  is time. The water table rise is

455 estimated as the difference between peak groundwater levels and the extrapolated antecedent

456 recession. The estimate of recharge from this method is sensitive to the estimate of the

457 specific yield.  $S_y$  is assumed to be 0.1 which is close to the measured effective porosity of the

458 Eastern View Formation (Love et al., 1993), and takes into account the presence of finer

459 sized sediments such as silt and clay in the aquifer. Annual water table fluctuations are

460 between 0.9 and 3.7 m across all bores, which for  $S_y$  values of 0.1, imply that  $R = 130$  to  $372$

461  $\text{mm yr}^{-1}$  in 2012 (mean of  $200 \text{ mm yr}^{-1}$ ) and  $90$  to  $300 \text{ mm yr}^{-1}$  in 2013 (mean of  $164 \text{ mm yr}^{-1}$ )

462 <sup>1</sup>). This equates to between 11 and 32 % of rainfall in 2012 and 12 and 28 % of rainfall in

463 2013. The bores are screened 11.2 to 42 m below the ground surface and thus these recharge

464 estimates will be minima due to the attenuation of pressure variations with depth (Scanlon et

465 al., 2002). Recharge estimates are also susceptible to the value of specific yield, particularly

466 where the aquifer is composed of finer sized sediments such as silt and clay. Regardless,

467 estimates using bore hydrographs indicate that significant groundwater recharge to the

468 unconfined Eastern View aquifer in the valley occurs via direct infiltration of precipitation.

469

470 (5.3) <sup>14</sup>C ages

471 As groundwater in the Eastern View Formation contains dissolved oxygen and nitrate  
 472 (Victorian Water Resources Data Warehouse, 2013),  $\delta^{13}\text{C}$  values are low, and there are no  
 473 reported occurrences of methane or coal seams within the Gellibrand River Catchment,  
 474 methanogenesis is unlikely to be a source of DIC. Likewise there are no obvious sources of  
 475 geogenic  $\text{CO}_2$  in this area. Based on the major ion geochemistry, only minor calcite  
 476 dissolution occurs in the Eastern View Formation, which is to be expected as the Cenozoic  
 477 aquifers are siliceous and contain only minor carbonate minerals. While only minor carbonate  
 478 dissolution is likely, determination of groundwater residence times requires this to be taken  
 479 into account. If it is assumed that closed system dissolution of calcite in the aquifers is the  
 480 major process, the fraction of C derived from the soil zone ( $q$ ) may be derived from the  $\delta^{13}\text{C}$   
 481 values of DIC ( $\delta^{13}\text{C}_{\text{DIC}}$ ), carbonate ( $\delta^{13}\text{C}_{\text{cc}}$ ) and recharging water ( $\delta^{13}\text{C}_r$ ) via Eq.(2):

482

$$483 \quad q = \frac{\delta^{13}\text{C}_{\text{DIC}} - \delta^{13}\text{C}_{\text{cc}}}{\delta^{13}\text{C}_r - \delta^{13}\text{C}_{\text{cc}}} \quad (2)$$

484

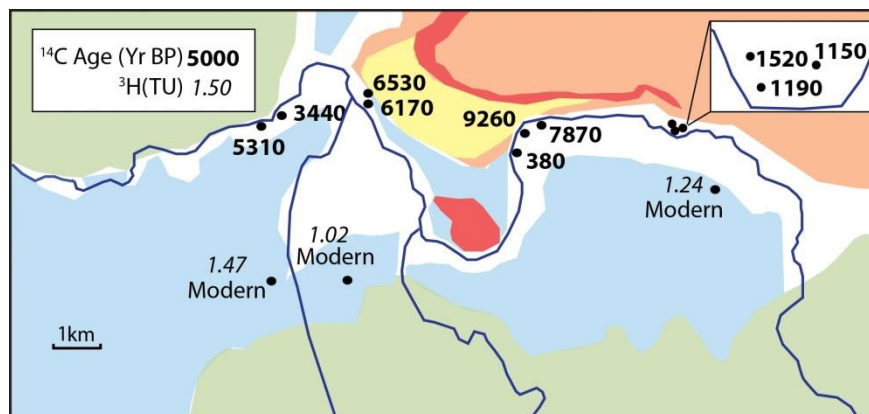
485 (Clark & Fritz 1997). The calcite is assumed to have a  $\delta^{13}\text{C}$  of  $\sim 0\text{‰}$  (Love et al., 1994;  
 486 Petrides and Cartwright, 2006) as is appropriate for marine sediments.  $\delta^{13}\text{C}_r$  is calculated  
 487 from the  $\delta^{13}\text{C}$  of the soil carbon in the recharge zone. Pre-land clearing vegetation in  
 488 southeast Australia was dominated by eucalypts that have  $\delta^{13}\text{C}$  values of  $-30$  to  $-27\text{‰}$  (Quade  
 489 et al., 1995). Assuming a  $\sim 4\text{‰}$   $^{13}\text{C}$  fractionation during outgassing (Cerling et al., 1991),  
 490  $\delta^{13}\text{C}$  values of soil  $\text{CO}_2$  would be  $-26$  to  $-23\text{‰}$  (average of  $-24.5\text{‰}$ ). At  $20^\circ\text{C}$  and pH 6.5,  
 491  $\delta^{13}\text{C}_r$  calculated from the fractionation data of Vogel et al. (1970) and Mook et al. (1974) is  
 492  $\sim -20\text{‰}$ . Although the calculated  $\delta^{13}\text{C}_r$  values require the pH and temperature of recharge  
 493 and the  $\delta^{13}\text{C}$  of the soil zone  $\text{CO}_2$  to be estimated, they are similar to those from other studies  
 494 in southeast Australia and consistent with the predicted  $\delta^{13}\text{C}$  values of DIC in equilibrium

495 with calcite in the regolith (Quade et al., 1995; Cartwright, 2010). Calculated q values are  
 496 between 0.85 and 0.97 (Table 2), implying that only 10% to 15% of DIC in groundwater  
 497 from the Eastern View formation is derived from calcite in the aquifer, this is similar to the  
 498 expected contribution of calcite dissolution in siliceous aquifers (Vogel et al., 1970) and  
 499 similar to other estimates from the Otway Basin (Love et al., 1994; Petrides and Cartwright,  
 500 2006).

501 Using the q values from Table 2,  $^{14}\text{C}$  ages (t) corrected for closed-system calcite dissolution  
 502 are calculated from Eq. (3); where  $a^{14}\text{C}$  is the activity of  $^{14}\text{C}$  in groundwater DIC, and  $a_o^{14}\text{C}$  is  
 503 the activity during recharge (assumed to be 100 pMC).

$$t = -8376 \ln \left( \frac{a^{14}\text{C}}{q \cdot a_o^{14}\text{C}} \right) \quad (3)$$

506 Radiocarbon ages for groundwater in the Eastern View Formation range from 380 to 9260  
 507 years (Table 2) with the exception of bores 5k, 5l and 5m which have  $a^{14}\text{C} > 100$  pMC and  
 508 represent groundwater that has a component of water recharged during or after the  
 509 atmospheric nuclear tests in the 1950s to 1960s. The majority of  $^{14}\text{C}$  ages however, suggest  
 510 that groundwater in the valley, especially in the near-river environment has long residence  
 511 times (Fig. 7).



517 **Figure 7** – Groundwater residence times within the Gellibrand Valley. Residence times up to 9260  
518 years are found in close proximity to the river. Modern local groundwaters with a  $^{14}\text{C}$  > 100 pMC are  
519 situated back on the floodplain. Data from Tables 1 and 2.

520 (5.4)  $^3\text{H}$  Activities and Recharge Rates

521 With a shorter half-life,  $^3\text{H}$  activities can infer the presence of modern groundwater. The  
522 water table fluctuations imply that the Gellibrand Valley receives considerable recharge year  
523 (90 to 370 mm yr $^{-1}$ ), and although head gradients at nested sites are upwards implying that  
524 the valley is a groundwater discharge zone (Fig. 2b), these may be reversed during periods of  
525 high rainfall. If local recharge is significant in recharging the groundwater system across the  
526 valley, it would be expected that the groundwater would have relatively high  $^3\text{H}$  activities.  
527 Recently-recharged groundwater in other Victorian catchments has  $^3\text{H}$  activities up to 3.6 TU  
528 (Cartwright & Morgenstern, 2012).

529

530  $^3\text{H}$  activities across most of the groundwater from the Gellibrand Valley are negligible, and  
531 with  $^{14}\text{C}$  ages of 380 to 9260 years, much of the groundwater is regional, originating from the  
532 Barongarook High. The exception to this is groundwater from the southern edge of the valley  
533 (Site 5) where the Eastern View Formation overlies the basement rock (Eumeralla Formation)  
534 and  $^3\text{H}$  activities and  $^{14}\text{C}$  activities are substantially higher than groundwater from sites 1 to 4.  
535 The mean residence times of water samples from the southern margin of the valley (Site 5)  
536 were evaluated from  $^3\text{H}$  activities using the TracerLPM Excel workbook (Jurgens et al.,  
537 2012). As the aquifer is unconfined throughout the valley, and bore screens sample only part  
538 of the aquifer, the partial exponential model (PEM) is applied, with the PEM ratio calculated  
539 for bores 5k, 5l and 5k as the ratio of the unsampled thickness of the aquifer to the sampled  
540 thickness (Jurgens et al., 2012). A value of 2.7 TU was used to represent modern and pre-  
541 bomb pulse rainfall based on the  $^3\text{H}$  activity of rainfall measured at Monash University and

542 expected  $^3\text{H}$  values in Southern Victoria (Tadros et al., 2014). For intervening years, the  
543 mean weighted average of  $^3\text{H}$  activities in precipitation in Melbourne was extracted from the  
544 International Atomic Energy Agency Melbourne record (International Atomic Energy  
545 Association, 2014). Calculated groundwater ages of 65 years (5k) 73 years (5l) and 59 years  
546 (5m) indicate that groundwater away from the river is modern and likely recharged from  
547 direct infiltration of precipitation. This supports  $\delta^{18}\text{O}$  and  $\delta^2\text{H}$  data which suggests that sites  
548 1 to 4 sample old, regional groundwater recharged on the Barongarook High, whilst site 5  
549 samples locally recharged groundwater within the valley. Although groundwater levels across  
550 sites 1 to 5 demonstrate annual recharge cycles, in the near-river environment (sites 1 to 4)  
551 much of the regional groundwater is from within 5 to 10 m of the water table, suggesting that  
552 any local recharge penetrates only to a limited depth, and does not mix with the bulk of the  
553 water in the Eastern View Formation. Conversely the high  $^3\text{H}$  activities and  $^{14}\text{C}$  activities at  
554 site 5, which occur in groundwater from depths of 21 – 42 m, imply that recharge to the  
555 deeper parts of the aquifer locally occurs at the southern edge of the floodplain.

556

557 The Gellibrand River has the potential to recharge regional groundwater during high river  
558 stages and episodic floods. Aquifer recharge from surface water can be assessed by  
559 combining data from groundwater EC values and  $^3\text{H}$  activities. The EC of river water varies  
560 between 120 and 200  $\mu\text{S cm}^{-1}$  and is lower than that of groundwater in the catchment  
561 throughout the year.  $^3\text{H}$  activities of river water are between 1.24 and 2.0 TU during baseflow  
562 conditions (Atkinson et al., 2013), and may be higher during high flow events as local  
563 modern rainfall (with  $^3\text{H}$  activities of 2.4 to 3.2 TU: Tadros et al., 2014) and relatively  
564 ‘young’ water draining the upper catchment likely comprise a significant component of river  
565 flow at those times. Significant amounts of aquifer recharge through overbank events or bank  
566 exchange should result in groundwater with low EC values, and high  $^3\text{H}$  activities near the



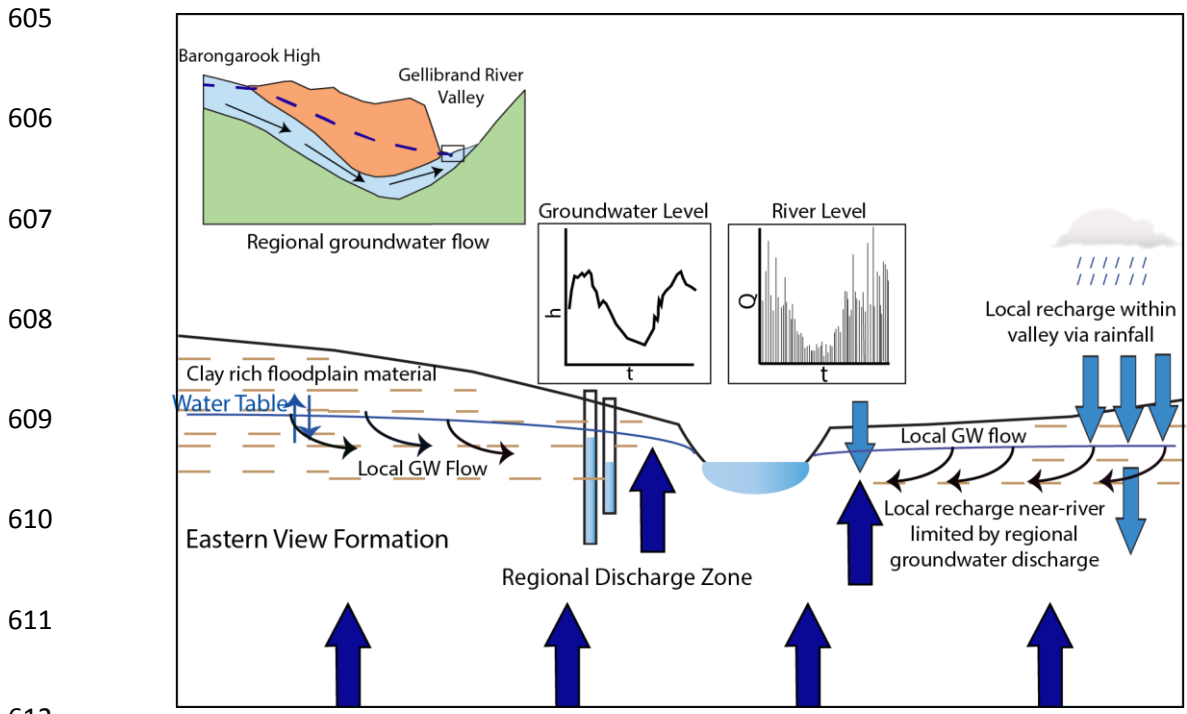
567 river. Except for in June 2012 when the bores were overtopped and a limited to response to  
568 high river flow events (June to July 2013), groundwater EC remains relatively constant  
569 throughout the study period and there is only a minor inverse relationship with river height  
570 (Fig. 6). This indicates there is little exchange of river water to the depth of the aquifer  
571 sampled by the bores. Additionally the activities of  $^3\text{H}$  in near-river bores are negligible,  
572 again suggesting that recharge from the river does not penetrate more than a few metres into  
573 the adjacent aquifer. Thus, flow through the river bank or river flooding does not appear to be  
574 a significant mechanism of recharge in the Gellibrand Valley. Instead, with upward head  
575 gradients and evidence for limited recharge in the near-river environment, the river likely acts  
576 as a groundwater discharge zone for the majority of the year, supplied by a combination of  
577 regional groundwater from the Barongarook High and local groundwater recharged within  
578 the valley.

579

#### 580 (5.5) Groundwater Flowpaths and Conceptual Model

581 Radiocarbon ages are up to 10 ka implying that the groundwater in the Gellibrand Valley has  
582 a long residence time; in turn this implies that the area is a regional discharge zone. Most of  
583 the groundwater originates on the Barongarook High, and this region potentially provides a  
584 substantial proportion of baseflow to the Gellibrand River. The large range of  $^{14}\text{C}$  ages in the  
585 Gellibrand Valley is a likely result of heterogeneous geology, where the presence of low  
586 hydraulic conductivity sediments such as silt and clays in the Eastern View Formation lead to  
587 variable velocities along groundwater flowpaths. Groundwater travel times may also be  
588 determined using the present day hydraulic gradients. From Darcy's law and assuming a  
589 porosity of 0.1 (Love et al., 1994) and a hydraulic conductivity of 0.2 to 2 m day $^{-1}$  (Love et  
590 al., 1993) calculated travel times are between 1000 and 10 000 years, which are similar to

591 those implied by the  $^{14}\text{C}$  ages. This and the depleted stable isotope signature of groundwater  
 592 samples from sites 1 to 4 supports the idea that groundwater in the valley is predominantly  
 593 regional groundwater derived by recharge on the Barongarook High. The high  $^3\text{H}$  activities in  
 594 groundwater bores from site 5 situated away from the river imply local recharge via  
 595 precipitation recharges the aquifer to depths of 21 to 42 m at the southern edge of the  
 596 floodplain. However for the most-part, shallow groundwater in the Gellibrand Valley,  
 597 including in the near-river environment is predominantly regional groundwater. Though  
 598 groundwater elevations display clear annual cycles and winter months are punctuated by high  
 599 river flow, localised recharge from both of these processes combined is stored in the upper 10  
 600 m of the aquifer. The infiltration of precipitation within the Gellibrand Valley is likely  
 601 limited by the presence of silts and clays on the floodplain and riverbanks. This is coupled  
 602 with strong upwards hydraulic gradients in the Eastern View Formation, driven by regional  
 603 groundwater flow from the Barongarook High, which ensure that recharge in the near-river  
 604 environment does not penetrate deep within the aquifer (Fig. 8).



613 **Figure 8** – Groundwater flow conceptualisation in the Gellibrand Valley. Though appreciable  
614 amounts of recharge are estimated from bore hydrographs and high river flows, the depth to which  
615 recharging waters infiltrate into the Eastern View Formation (downward leakage) is limited by strong  
616 upward head gradients, and a floodplain which consists of appreciable amounts of silt and clay.

617 (5.6)  $^{14}\text{C}$  ages & Cl

618 The good correlation of a  $^{14}\text{C}$  with chloride implies that chloride concentrations correspond to  
619 groundwater age (Fig. 9). Correlations between  $^{14}\text{C}$  and Cl have also been documented in  
620 groundwater from the Eastern View Formation in other regions of the Otway Basin (Love et  
621 al., 1994). In assessing this relationship, chloride sources must be considered. That the Cl/Br  
622 ratios in the groundwater are similar to those of rainfall preclude significant halite dissolution  
623 by the groundwater from the Eastern View Formation, and there are no extensive occurrences  
624 of halite in the aquifer matrix.

625

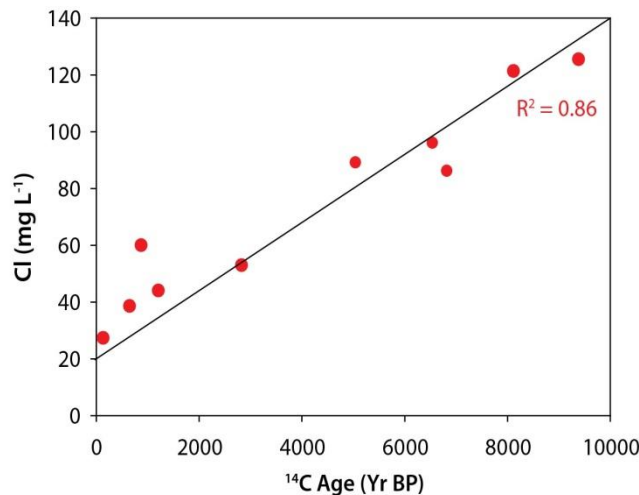
626

627

628

629

630



631 **Figure 9** –  $^{14}\text{C}$  age v Cl.  $^{14}\text{C}$  ages are taken from the calcite corrected ages in *Table 1*

632

633 We propose three possible explanations of this trend. Firstly, the relationship between a  $^{14}\text{C}$   
634 and Cl may be explained by mixing of low salinity groundwater that is locally recharged  
635 within the valley (Site 5) and high salinity regional groundwater from the Barongarook High

636 (Sites 1 to 4). However, groundwater samples from site 5 which have high  $a^{14}\text{C}$  and low Cl  
637 also have high  $^3\text{H}$  activities (0.99 to 1.47 TU) suggesting if mixing has occurred it must do so  
638 at a very slow rate otherwise the resultant groundwater (Sites 1 to 4) would be expected to  
639 contain measurable  $^3\text{H}$ . This implies that mixing between the shallow groundwater system  
640 and the deeper groundwater is limited.

641

642 It is possible that the Cl concentrations in groundwater preserve a record of climate  
643 variability. In the Otway Basin Love et al. (1994) report a decrease in Cl concentrations in  
644 groundwater recharged between 18 and 10 ka, followed by an increase in Cl concentrations in  
645 groundwater recharged from 10 ka to the present day, which they attribute to increased  
646 evapotranspiration rates during a warming Holocene climate. However, in this study  
647 decreasing Cl concentrations with increasing  $a^{14}\text{C}$  would imply that recharge rates on the  
648 Barongarook high increased from 10,000 years BP to the present, which is not likely given  
649 the warming trend over that period.

650

651 It is more likely that the correlation between  $a^{14}\text{C}$  and Cl concentrations reflects spatially  
652 variable recharge on the Barongarook High due to the heterogeneous sediments within the  
653 Eastern View Formation. Evapotranspiration during recharge is commonly the dominant  
654 process in determining the salinity of groundwater in SE Australia (Herczeg et al., 2001).  
655 Low recharge rates result in higher degrees of evapotranspiration and higher salinity  
656 groundwater, and the resultant correlation between Cl concentrations and  $^{14}\text{C}$  ages has been  
657 noted in other catchments (Leaney et al., 2003; Cartwright et al., 2006). Variable recharge  
658 rates could result in a wide range of recharge ages in the Gellibrand Valley, with the high Cl  
659 low  $a^{14}\text{C}$  groundwater being derived from regions with locally low recharge rates. Regardless

660 of which model is correct, the chloride measurements provide a useful first order estimate of  
661 groundwater residence times.

## 662 **(6) Conclusion**

663 Though widely available water-table measurements offer an insight into recharge, the  
664 dynamics of groundwater flow systems and recharge patterns can only be fully understood  
665 when combined with geochemical data, in particular radiogenic tracers such as  $^3\text{H}$  and  $^{14}\text{C}$ .  
666 These can be used to assess the importance of recharge and discharge in aquifer windows,  
667 which in turn defines groundwater pathways and allows the potential fate of pollutants to be  
668 assessed. Here shallow (11 to 42 m) groundwater bores indicate a significant amount of  
669 recharge occurs in the Gellibrand River Valley (90 to 370 mm yr<sup>-1</sup>). However, the  
670 groundwater at 5 to 10 m below the water table has  $^{14}\text{C}$  ages between 350 and 10,000 years,  
671 and below detection  $^3\text{H}$  activities. Furthermore, there is no indication of water from the river  
672 penetrating more than ~10 m following flood events. In the Gellibrand River Valley,  
673 outcropping aquifer sediments act as a regional discharge zone. Upwards head gradients are  
674 maintained for long periods of time and aided by the presence of silts and clays on the  
675 floodplain, this limits the depth to which diffuse and localised recharge (via over-bank events  
676 and bank exchange) penetrate the aquifer.

677

678 There is most likely a shallow local flow system within the Gellibrand River Valley that has  
679 limited connectivity with the deeper groundwater, particularly in the near-river environment.  
680 This potentially limits the spread of pollutants such as nitrate and pesticides that may derive  
681 from the agricultural activities into the regional groundwater. Future land-use, climate change  
682 or groundwater exploitation that occurs on the Barongarook High or in the Gellibrand River

683 Catchment is likely to affect both the chemistry of groundwater and groundwater fluxes to the  
684 Gellibrand River, highlighting the importance of protecting regional recharge zones.

685

## 686 **Acknowledgements**

687

688 We would like to thank colleagues who assisted in laboratory analysis. In particular,  
689 Massimo Raveggi and Rachelle Pierson (Monash University) for stable isotope, anion and  
690 cation analyses, and Simon Varley (ANSTO) for  $^{14}\text{C}$  determinations.

691

## 692 **References**

693

694 Alley, W.M., Healy, R.W., LaBaugh J.W., and Reilly, T.E.: Flow and storage in groundwater  
695 systems. (Review: hydrology). *Science*, 296: 1985-1990 DOI:10.1126/science.106712,  
696 2002.

697

698 Aravena, R., Leonard, I., Wassenaar, L., and Plummer, N.: Estimating  $^{14}\text{C}$  Groundwater  
699 Ages in a Methanogenic Aquifer. *Water Resour Res*, 9: 2307-2317. DOI:  
700 10.1029/95WR01271, 1995.

701

702 Atkinson, A.P., Cartwright, I., Gilfedder, B.S., Hofmann, H., Unland, N.P., Cendón, D.I., and  
703 Chisari, R.: A multi-tracer approach to quantifying groundwater inflows to an upland  
704 river; assessing the influence of variable groundwater chemistry. *Hydrol Process*.  
705 Available Online. DOI: 10.1002/hyp.10122, 2013.

706

707 Bennetts, D.A., Webb, J.A., Stone, D.J.M., and Hill, D.M.: Understanding the salinisation  
708 process for groundwater in an area of south-eastern Australia, using hydrochemical

709 and isotopic evidence. J Hydrol, 323: 178-192. DOI:  
710 <http://dx.doi.org/10.1016/j.jhydrol.2005.08.023>, 2006.

711

712 Bertrand, G., Celle-Jeanton, H., Loock, S., Huneau, F., Lavastre, V.: Contribution of  
713  $\delta^{13}\text{C}$ ICITD and PCO<sub>2</sub> eq measurements to the understanding of groundwater  
714 mineralization and carbon patterns in volcanic aquifers. Application to Argnat Basin  
715 (Massif Central). Aq. Geochem. 19 (2): 147-171. DOI: 10.1007/s10498-012-9185-0,  
716 2013.

717

718 Bethke, C.M. and Johnson, T.M.: Groundwater Age and Groundwater Age Dating. Annual  
719 Review of Earth Planet Sc Lett, 36: 121-152. DOI:  
720 0.1146/annurev.earth.36.031207.124210, 2008.

721

722 Blackburn, G. and Mcleod, S.: Salinity of atmospheric precipitation in the Murray-Darling  
723 drainage division, Australia. Soil Research, 21: 411-434. DOI:  
724 <http://dx.doi.org/10.1071/SR9830411>, 1983.

725

726 Böhlke, J.K. and Denver, J.M.: Combined Use of Groundwater Dating, Chemical, and  
727 Isotopic Analyses to Resolve the History and Fate of Nitrate Contamination in Two  
728 Agricultural Watersheds, Atlantic Coastal Plain, Maryland. Water Resour Res, 31:  
729 2319-2339. DOI: 10.1029/95wr01584, 1995.

730

731 Böhlke, J.K.: Groundwater recharge and agricultural contamination. Hydrogeol J, 10: 153-  
732 179. DOI: 10.1007/s10040-001-0183-3, 2002.

733

734 Briguglio, D., Kowalczyk, J., Stilwell, J.D., Hall, M., and Coffa, A.: Detailed  
735 paleogeographic evolution of the Bass Basin: Late Cretaceous to present. Aust Journal  
736 Earth Sci, 60: 719-734. DOI: 10.1080/08120099.2013.826282, 2013.

737

738 Bureau of Meteorology, 2013. Commonwealth of Australia Bureau of Meteorology.  
739 <http://www.bom.gov.au>, last access: 14 January 2014.

740

741 Campana, M.E. and Simpson, E.S.: Groundwater residence times and recharge rates using a  
742 discrete-state compartment model and <sup>14</sup>C data. J Hydrol, 72: 171-185. DOI:  
743 [http://dx.doi.org/10.1016/0022-1694\(84\)90190-2](http://dx.doi.org/10.1016/0022-1694(84)90190-2), 1984.

744

745 Cardenas, M.B.: Potential contribution of topography-driven regional groundwater flow to  
746 fractal stream chemistry: Residence time distribution analysis of Tóth flow. Geophys  
747 Res Lett, 34: L05403. DOI: 10.1029/2006gl029126, 2007.

748

749 Cartwright, I., Weaver, T.R., and Fifield, L.K.: Cl/Br ratios and environmental isotopes as  
750 indicators of recharge variability and groundwater flow: An example from the  
751 southeast Murray Basin, Australia. Chem. Geol, 231: 38-56. DOI:  
752 <http://dx.doi.org/10.1016/j.chemgeo.2005.12.009>, 2006.

753

754 Cartwright, I. and Morgenstern, U.: Constraining groundwater recharge and the rate of  
755 geochemical processes using tritium and major ion geochemistry: Ovens catchment,  
756 southeast Australia. J Hydrol, 475: 137-149. DOI:  
757 <http://dx.doi.org/10.1016/j.jhydrol.2012.09.037>, 2012.

758

759 Cartwright, I., Weaver, T.R., Cendón, D.I., Fifield, L.K., Tweed, S.O., Petrides, B., and  
760 Swane I.: Constraining groundwater flow, residence times, inter-aquifer mixing, and  
761 aquifer properties using environmental isotopes in the southeast Murray Basin,  
762 Australia. Appl Geochem, 27: 1698-1709. DOI:  
763 <http://dx.doi.org/10.1016/j.apgeochem.2012.02.006>, 2012.

764



765 Cartwright, I., Fifield, L.K., and Morgenstern, U.: Using  $^3\text{H}$  and  $^{14}\text{C}$  to constrain the degree of  
766 closed-system dissolution of calcite in groundwater. *App Geochem*, 32: 118-128. DOI:  
767 <http://dx.doi.org/10.1016/j.apgeochem.2012.10.023>, 2013.

768

769 Cendón, D.I., Larsen, J.R., Jones, B.G., Nanson, G.C., Rickleman, D., Hankin, S.I., Pueyo,  
770 J.J., and Maroulis, J.: Freshwater recharge into a shallow saline groundwater system,  
771 Cooper Creek floodplain, Queensland, Australia. *J Hydrol*, 392: 150-163. DOI:  
772 <http://dx.doi.org/10.1016/j.jhydrol.2010.08.003>, 2010.

773 Cendón, D.I., Hankin, S.I., Williams, J.P., Van Der Ley, M., Peterson, M., Hughes, C.E.,  
774 Meredith, K., Graham, I.T., Hollins, S.E., Levchenko, V., and Chisari, R.:  
775 Groundwater residence time in a dissected and weathered sandstone plateau: Kulnura-  
776 Mangrove Mountain aquifer, NSW, Australia. *Aust J of Earth Sci*, 1-25  
777 <http://dx.doi.org/10.1080/0812099.2014.894628>, 2014.

778

779 Cerling, T.E., Solomon, D.K., Quade, J., and Bowman, J.R.: On the isotopic composition of  
780 carbon in soil carbon dioxide. *Geochim Cosmochim Ac*, 55: 3403-3405. DOI:  
781 [http://dx.doi.org/10.1016/0016-7037\(91\)90498-T](http://dx.doi.org/10.1016/0016-7037(91)90498-T), 1991.

782

783 Chen, X. and Chen, X.: Stream water infiltration, bank storage, and storage zone changes due  
784 to stream-stage fluctuations. *J Hydrol*, 280: 246-264. DOI:  
785 [http://dx.doi.org/10.1016/S0022-1694\(03\)00232-4](http://dx.doi.org/10.1016/S0022-1694(03)00232-4), 2003.

786

787

788 Clark, I.D. and Fritz, P.: *Environmental Isotopes in Hydrogeology*. Lewis, New York, USA,  
789 1997.

790

791 Cook, P., Herczeg, A., and Kalin, R.: Radiocarbon Dating of Groundwater Systems. In:  
792 *Environmental Tracers in Subsurface Hydrology*, Springer US, pp: 111-144, 2000.

793

794 Cook, P.G. and Robinson, N.I.: Estimating groundwater recharge in fractured rock from  
795 environmental  $^3\text{H}$  and  $^{36}\text{Cl}$ , Clare Valley, South Australia. *Water Res Res*, 38: 11-11-  
796 11-13. DOI: 10.1029/2001wr000772, 2002.

797

798 Coplen, T.B.: Normalization of oxygen and hydrogen isotope data. *Chem. Geol.*, 72: 293-297.  
799 DOI: 10.1016/0168-9622(88)90042-5, 1988.

800 Dansgaard, W.: Stable isotopes in precipitation. *Tellus.*, 16 (4): 436-468.

801 DOI:10.1111/j.2153-3490.1964.tb00181.x, 1964.

802

803 Doble, R.B.P., McCallum, J., and Cook, P.: An analysis of river bank slope and unsaturated  
804 flow effect on bank storage. *Groundwater*, 50: 77-86. DOI: 0.1111/j.1745-  
805 6584.2011.00821.x, 2012.

806

807 Edmunds, W.M., Carrillo-Rivera, J.J., and Cardona, A.: Geochemical evolution of  
808 groundwater beneath Mexico City. *J Hydrol*, 258: 1-24. DOI:  
809 [http://dx.doi.org/10.1016/S0022-1694\(01\)00461-9](http://dx.doi.org/10.1016/S0022-1694(01)00461-9), 2002.

810

811 Fink, D., Hotchkis, M., Hua, Q., Jacobsen, G., Smith, A.M., Zoppi, U., Child, D., Mifsud, C.,  
812 van der Gaast, H., Williams, A., and Williams, M.: The ANTARES AMS facility at  
813 ANSTO. *Nuclear Instruments and Methods in Physics Research B* 223-224, 109-115,  
814 2004.

815

816 Foster, S.S.D., and Chilton, P.J.: Groundwater: the processes and global significance of  
817 aquifer degradation. *Philosophical Transactions of the Royal Society of London*  
818 *Series B-Biological Sciences*, 358: 1957-1972. DOI: 10.1098/rstb.2003.1380, 2003.

819

820 Frederico, C., Aiuppa, A., Allad, P., Bellomo, S., Jean-Baptiste, P., Parello, F., Valenza, M.:  
821 Magma-derived gas influx and water-rock interactions in the volcanic aquifer of Mt  
822 Vesuvius, Italy. *Geochim. Cosmochim. Acta*, 66(6): 963-981, 2002.

823

824 Frisbee, M.D., Wilson, J.L., Gomez-Velez, J.D., Phillips, F.M., and Campbell, A.R.: Are we  
825 missing the tail (and the tale) of residence time distributions in watersheds? *Geophys*  
826 *Res Lett*, 40: 4633-4637. DOI: 10.1002/grl.50895, 2013.

827 Gardner, W.P., Harrington, G.A., Solomon, D.K., and Cook, P.G.: Using terrigenic <sup>4</sup>He to  
828 identify and quantify regional groundwater discharge to streams. *Water Resour Res*,  
829 47: W06523. DOI: 10.1029/2010wr010276, 2011.

830

831 Goderniaux, P., Davy, P., Bresciani, E., de Dreuzuy, J.R., and Le Borgne, T.: Partitioning a  
832 regional groundwater flow system into shallow local and deep regional flow  
833 compartments. *Water Resour Res*, 49: 2274-2286. DOI: 10.1002/wrcr.20186, 2013.

834

835 Han, L.F. and Plummer, L.N.: Revision of Fontes & Garnier's model for the initial <sup>14</sup>C  
836 content of dissolved inorganic carbon used in groundwater dating. *Chem. Geol.*, 351:  
837 105-114. DOI: <http://dx.doi.org/10.1016/j.chemgeo.2013.05.011>, 2013.

838

839 Herczeg, A.L., Dogramaci, S.S., and Leaney, F.W.J.: Origin of dissolved salts in a large,  
840 semi-arid groundwater system: Murray Basin, Australia. *Mar. Freshw. Res.*, 52: 41-52.  
841 DOI: <http://dx.doi.org/10.1071/MF00040>, 2001.

842

843 Hilscherova, K., Dusek, L., Kubik, V., Cupr, P., Hofman, J., Klanova, J., and Holoubek, I.:  
844 Redistribution of organic pollutants in river sediments and alluvial soils related to  
845 major floods. *Journal of Soils and Sediments*, 7: 167-177. DOI:  
846 10.1065/jss2007.04.222, 2007.

847

848 Hortle, A., de Caritat, P., Stalvies, C., and Jenkins, C.: Groundwater monitoring at the Otway  
849 project site, Australia. *Energy Procedia*, 4: 5495-5503. DOI:  
850 <http://dx.doi.org/10.1016/j.egypro.2011.02.535>, 2011.

851

852 Hughes, C.E. and Crawford, J.: A new precipitation weighted method for determining the  
853 meteoric water line for hydrological applications demonstrated using Australian and  
854 global GNIP data. *J Hydrol*, 464: 344-351. DOI:  
855 <http://dx.doi.org/10.1016/j.jhydrol.2012.07.029>, 2012.

856

857 Jurgens B.C., Böhlke J.K., Eberts S.M.: TracerLPM (Version 1): An Excel® workbook for  
858 interpreting groundwater age distributions from environmental tracer data: U.S.  
859 Geological Survey Techniques and Methods Report 4- F3, 60p, 2012.

860

861 Krüger, F., Meissner, R., Gröngröft, A., and Grunewald, K.: Flood Induced Heavy Metal and  
862 Arsenic Contamination of Elbe River Floodplain Soils. *Acta hydroch hydrob*, 33:  
863 455-465. DOI: 10.1002/aheh.200400591, 2005.

864

865 Leaney, F.W., Herczeg, A.K., Walker, G.R.: Stable isotope geochemistry of ground and  
866 surface waters associated with undisturbed massive sulphide deposits; constraints on  
867 origin of waters and water-rock reactions. *Chemical Geology*, 2006.

868

869 Leonard, J., Lakey, R., and Cumming, S.: Gellibrand groundwater investigation interim  
870 report. Geologic Survey of Victoria. Department of Minerals and Energy.  
871 Unpublished Report, 1981

872

873 Le Gal La Salle, C., Marlin, C., Leduc, C., Taupin, J.D., Massault, M., and Favreau, G.:  
874 Renewal rate estimation of groundwater based on radioactive tracers (<sup>3</sup>H, <sup>14</sup>C) in an

875 unconfined aquifer in a semi-arid area, Iullemeden Basin, Niger. J Hydrol, 254: 145-  
876 156. DOI: [http://dx.doi.org/10.1016/S0022-1694\(01\)00491-7](http://dx.doi.org/10.1016/S0022-1694(01)00491-7), 2001.

877

878 Love, A.J., Herczeg, A.L., Armstrong, D., Stadter, F., and Mazor, E.: Groundwater flow  
879 regime within the Gambier Embayment of the Otway Basin, Australia: evidence from  
880 hydraulics and hydrochemistry. J Hydrol, 143: 297-338. DOI:  
881 [http://dx.doi.org/10.1016/0022-1694\(93\)90197-H](http://dx.doi.org/10.1016/0022-1694(93)90197-H), 1993.

882 Love, A.J., Herczeg, A.L., Leaney, F.W., Stadter, M.F., Dighton, J.C., and Armstrong, D.:  
883 Groundwater residence time and palaeohydrology in the Otway Basin, South  
884 Australia:  $^2\text{H}$ ,  $^{18}\text{O}$  and  $^{14}\text{C}$  data. J Hydrol, 153: 157-187. DOI:  
885 [http://dx.doi.org/10.1016/0022-1694\(94\)90190-2](http://dx.doi.org/10.1016/0022-1694(94)90190-2), 1994.

886

887 Manning, A.H., Clark, J.F., Diaz, S.H., Rademacher, L.K., Earman, S., and Plummer, N.L.:  
888 Evolution of groundwater age in a mountain watershed over a period of thirteen years.  
889 J Hydrol, 460: 13-28. DOI: <http://dx.doi.org/10.1016/j.jhydrol.2012.06.030>, 2012.

890

891 Mazor, E., and Nativ, R.: Hydraulic calculation of groundwater flow velocity and age:  
892 examination of the basic premises. J Hydrol, 138: 211-222. DOI:  
893 [http://dx.doi.org/10.1016/0022-1694\(92\)90165-R](http://dx.doi.org/10.1016/0022-1694(92)90165-R), 1992.

894

895 McCallum, J.L., Cook, P.G., Brunner, P., and Berhane, D.: Solute dynamics during bank  
896 storage flows and implications for chemical base flow separation. Water Resour. Res.,  
897 46: W07541. DOI: 10.1029/2009wr008539, 2010.

898

899 McDonnell, J.J., McGuire, K., Aggarwal, P., Beven, K.J., Biondi, D., Destouni, G., Dunn, S.,  
900 Kirchner, J.A., Kraft, P., Lyon, S., Maloszewski, P., Newman, B., Pfister, L., Rinaldo,  
901 A., Rodhe, A., Sayama, T., Seibert, J., Solomon, K., Soulsby, C., Stewart, M.,  
902 Tetzlaff, D., Tobin, C., Troch, P., Weiler, M., Western, A., Wörman, A., and Wrede,

903 S.: How old is streamwater? Open questions in catchment transit time  
904 conceptualization, modelling and analysis. *Hydrol Process*, 24: 1745-1754. DOI:  
905 10.1002/hyp.7796, 2010.

906

907 Meredith, K.T., Cendón, D.I., Pigois, J-P., Hollins, S.E., and Jacobsen, G.: Using  $^{14}\text{C}$  and  $3\text{H}$   
908 to delineate a recharge 'window' into the Perth Basin aquifers, North Gngangara  
909 groundwater system, Western Australia. *Sci Total Environ*, 414, 456-469, 2012.

910 Michel, R.L.: Tritium hydrology of the Mississippi River basin. *Hydrol Process*, 18: 1255-  
911 1269. DOI: 10.1002/hyp.1403, 2004.

912

913 Moench, A.F. and Barlow, P.M.: Aquifer response to stream-stage and recharge variations. I.  
914 Analytical step-response functions. *J Hydrol*, 230: 192-210. DOI:  
915 [http://dx.doi.org/10.1016/S0022-1694\(00\)00175-X](http://dx.doi.org/10.1016/S0022-1694(00)00175-X), 2000.

916

917 Mook, W.G., Bommerson, J.C., and Staverman, W.H.: Carbon isotope fractionation between  
918 dissolved bicarbonate and gaseous carbon dioxide. *Earth Planet Sc Lett*, 22: 169-176.  
919 DOI: [http://dx.doi.org/10.1016/0012-821X\(74\)90078-8](http://dx.doi.org/10.1016/0012-821X(74)90078-8), 1974.

920

921 Morgenstern, U. and Taylor, C.B.: Ultra low-level tritium measurement using electrolytic  
922 enrichment and LSC. *Isot environ and health s*, 45(2) 96-117, 2009.

923

924 Morgenstern, U. Stewart, M.K., and Stenger, R.: Dating of streamwater using tritium in a  
925 post nuclear bomb pulse world: continuous variation of mean transit time with  
926 streamflow. *Hydrol. Earth Syst. Sci.*, 14: 2289-2301. DOI: 10.5194/hess-14-2289-  
927 2010.

928

929 Muennich, K.O.: Messung des <sup>14</sup>C-Gehaltes von hartem Grundwasser. Naturwissenschaften  
930 34, 32-33, 1957.

931

932 Neklapilova, B.: Conductivity measurements and large volumes distillation of samples for  
933 Tritium analysis. ANSTO internal guideline. Technical Report ENV-I-070-002,  
934 ANSTO – Institute for Environmental Research, Australia, 2008a.

935 Neklapilova, B.: Electrolysis and small volume distillation of samples for tritium activity  
936 analysis, ANSTO internal guideline. Technical Report ENV-I-070-003, ANSTO –  
937 Institute for Environmental Research, Australia, 2008b.

938

939 Newsom, J.M. and Wilson, J.L.: Flow of Ground Water to a Well Near a Stream – Effect of  
940 Ambient Ground-Water Flow Direction. Ground Water, 26: 703-711. DOI:  
941 10.1111/j.1745-6584.1988.tb00420.x, 1988.

942

943 Payton Gardner, W., Susong, D.D., Kip Solomon, D., and Heasler, H.: Snowmelt hydrograph  
944 interpretation: Revealing watershed scale hydrologic characteristics of the  
945 Yellowstone volcanic plateau. J Hydrol, 383: 209-222. DOI:  
946 <http://dx.doi.org/10.1016/j.jhydrol.2009.12.037>, 2010.

947

948 Petrides, B. and Cartwright, I.: The hydrogeology and hydrogeochemistry of the Barwon  
949 Downs Graben aquifer, southwestern Victoria, Australia. Hydrogeol J, 14: 809-826.  
950 DOI: 10.1007/s10040-005-0018-8, 2006.

951

952 Post, V.E.A., Vandenbohede, A., Werner, A.D., Maimun, S., and Teubner, M.D.:  
953 Groundwater ages in coastal aquifers. *Adv in Water Resour*, 57: 1-11. DOI:  
954 <http://dx.doi.org/10.1016/j.advwatres.2013.03.011>, 2013.

955

956 Quade, J., Chivas, A.R., and McCulloch, M.T.: Strontium and carbon isotope tracers and the  
957 origins of soil carbonate in South Australia and Victoria. *Palaeogeogr Palaeocl*, 113:  
958 103-117. DOI: [http://dx.doi.org/10.1016/0031-0182\(95\)00065-T](http://dx.doi.org/10.1016/0031-0182(95)00065-T), 1995.

959

960 Reilly, T.E., Plummer, L.N., Phillips, P.J., and Busenberg, E.: The use of simulation and  
961 multiple environmental tracers to quantify groundwater flow in a shallow aquifer.  
962 *Water Resour Res*, 30: 421-433. DOI: 10.1029/93wr02655, 1994.

963

964 Samborska, K., Rózkowski, A., and Małozzewski, P.: Estimation of groundwater residence  
965 time using environmental radioisotopes ( $^{14}\text{C}$ , T) in carbonate aquifers, southern  
966 Poland. *Isot Environ Healt St*, 49: 73-97. DOI: 10.1080/10256016.2012.677041, 2012.

967

968 Scanlon, B., Healy, R., and Cook, P.: Choosing appropriate techniques for quantifying  
969 groundwater recharge. *Hydrogeol J*, 10: 18-39. DOI: 10.1007/s10040-001-0176-2,  
970 2002.

971

972 Shentsis, I. and Rosenthal, E.: Recharge of aquifers by flood events in an arid region. *Hydrol*  
973 *Process*17: 695-712. DOI: 10.1002/hyp.1160, 2003.

974

975 Sklash. M.G. and Farvolden, R.N.: The role of groundwater in storm runoff. *J Hydrol*, 43: 45-  
976 65. DOI: [http://dx.doi.org/10.1016/0022-1694\(79\)90164-1](http://dx.doi.org/10.1016/0022-1694(79)90164-1), 1979.

977



978 Smerdon, B.D., Payton Gardner, W., Harrington, G.A., and Tickell, S.J.: Identifying the  
979 contribution of regional groundwater to the baseflow of a tropical river (Daly River,  
980 Australia). J Hydrol, 464-465: 107-115. DOI:  
981 <http://dx.doi.org/10.1016/j.jhydrol.2012.06.058>, 2012.

982

983 Stewart, M.K.: A 40-year record of carbon-14 and tritium in the Christchurch groundwater  
984 system, New Zealand: Dating of young samples with carbon-14. J Hydrol, 430: 50-68.  
985 DOI: <http://dx.doi.org/10.1016/j.jhydrol.2012.01.046>, 2012.

986

987 Stichler, W., Maeszewski, P., and Moser, H.: Modelling of river water infiltration using  
988 oxygen-18 data. J Hydrol, 83: 355-365. DOI: [http://dx.doi.org/10.1016/0022-  
989 1694\(86\)90161-7](http://dx.doi.org/10.1016/0022-1694(86)90161-7), 1986.

990

991 Stuvier, M. And Polach, H.A.: Reporting of <sup>14</sup>C data. Radiocarbon, 19: 355-363, 1977.

992

993 Stuyfzand, P.J.: Hydrology and water quality aspects of rhine bank groundwater in The  
994 Netherlands. J Hydrol, 106: 341-363. DOI: [http://dx.doi.org/10.1016/0022-  
995 1694\(89\)90079-6](http://dx.doi.org/10.1016/0022-1694(89)90079-6), 1989.

996

997 Tadros, C.V., Hughes, C.E., Crawford, J., Hollins, S.E., and Chisari, R.: Tritium in Australian  
998 Precipitation: a 50 Year Record. J Hydrol. DOI:  
999 <http://dx.doi.org/10.1016/j.jhydrol.2014.03.031>, 2014.

1000

1001 Tesoriero, A.J., Spruill, T.B., Mew, H.E., Farrell, K.M., and Harden, S.L.: Nitrogen transport  
1002 and transformations in a coastal plain watershed: Influence of geomorphology on flow  
1003 paths and residence times. Water Resour Res, 41: W02008. DOI:  
1004 10.1029/2003wr002953, 2005.

1005

1006 Tóth, J.: A theoretical analysis of groundwater flow in small drainage basins. *J Geophys Res*,  
1007 68: 4795-4812. DOI: 10.1029/JZ068i016p04795, 1963.

1008

1009

1010 Unland, N.P., Cartwright, I., Cendón, D.I., and Chisari, R.: Residence times and mixing of  
1011 water in river banks: implications for recharge and groundwater &ndash; surface  
1012 water exchange. *Hydrol. Earth Syst. Sci. Discuss.*, 11: 1651-1691. DOI:  
1013 10.5194/hessd-11-1651-2014, 2014.

1014

1015 Van den Berg, A.H.M., Rock unit names in western Victoria, Seamless Geology Project.  
1016 Geological Survey of Victoria Report 130. GeoScience Victoria, State of Victoria,  
1017 Department of Primary Industries, 2009.

1018

1019 Victorian Water Resources Data Warehouse: Victorian Department of Sustainability and  
1020 Environment Water Resources Data Warehouse, available at  
1021 <http://www.vicwaterdata.net>, last access: January 2014.

1022

1023 Vogel, J.C., Grootes, P.M., and Mook, W.G.: Isotopic fractionation between gaseous and  
1024 dissolved carbon dioxide. *Z. Physik*, 230: 225-238. DOI: 10.1007/bf01394688, 1970.

1025

1026 Vogel, J.C., Thilo, L., and Van Dijken, M.: Determination of groundwater recharge with  
1027 tritium. *J Hydrol*, 23: 131-140. DOI: [http://dx.doi.org/10.1016/0022-1694\(74\)90027-4](http://dx.doi.org/10.1016/0022-1694(74)90027-4),  
1028 1974.

1029

1030 Vogt, T., Hoehn, E., Schneider, P., Freund, A., Schirmer, M., and Cirpka, O.A.: Fluctuations  
1031 of electrical conductivity as a natural tracer for bank filtration in a losing stream. *Adv*

1032 Water Resour, 33: 1296-1308. DOI:  
1033 <http://dx.doi.org/10.1016/j.advwatres.2010.02.007>, 2010.  
1034  
1035 Wigley, T.M.L.: Carbon 14 dating of groundwater from closed and open systems. Water  
1036 Resour Res, 11: 324-328. DOI: 10.1029/WR011i002p00324, 1975.  
1037  
1038 Zhai, Y., Wang, J., Teng, Y., and Zuo, R.: Hydrogeochemical and isotopic evidence of  
1039 groundwater evolution and recharge in aquifers in Beijing Plain, China.  
1040 Environmental Earth Sciences, 69: 2167-2177. DOI: 10.1007/s12665-012-2045-9,  
1041 2013.

**Table 1** – Screen depth, Cl, <sup>18</sup>O, <sup>2</sup>H, <sup>13</sup>C, a<sup>14</sup>C and <sup>3</sup>H activities of groundwater samples. <sup>a</sup>Refers to bore name on the Victorian Water Resources Data Warehouse. <sup>b</sup> Measured as depth to the middle of the well screen. <sup>c</sup><sup>3</sup>H activities that are below detection.

Sample No.	Screen Depth (m)	EC (µS cm <sup>-1</sup> )	Cl	Br	Na	Ca	Mg	K	HCO <sub>3</sub> <sup>-</sup>	SO <sub>4</sub> <sup>2-</sup>	δ <sup>18</sup> O (‰VSMOW)	δ <sup>2</sup> H (‰VSMOW)	δ <sup>13</sup> C <sub>DIC</sub> (‰PDB)	a <sup>14</sup> C		<sup>3</sup> H	
														pMC	1σ	TU	1σ
<b>1a</b> (108899) <sup>a</sup>	29 <sup>b</sup>	282	60	0.18	35.1	4.8	2.9	2.2	0.23	0.14	-5.6	-32.7	-21.4	81	0.34	<i>bd</i> <sup>c</sup>	-
<b>1b</b> (108916)	14.5	197	38.6	0.12	29.3	3.4	4.1	1/9	0.24	0.09	-5.3	-30.4	-22.1	83.3	0.28	<i>bd</i>	-
<b>1c</b> (108917)	14.5	238	44	0.08	20.3	1.0	2.6	0.7	0.44	0.08	-5.3	-31.1	-21.5	77.8	0.29	<i>bd</i>	-
<b>2d</b> (108927)	14	430	86	0.07	69.1	16.3	9.9	7.4	0.5	0.36	-5.6	-32	-20	39.5	0.2	<i>bd</i>	-
<b>2e</b> (108928)	17	446	96	0.08	76.3	19.9	11	8.6	0.58	0.27	-5.5	-33.6	-19.8	40.9	0.21	<i>bd</i>	-
<b>3f</b> (108933)	11.2	491	121	0.1	84	8.6	5.3	9.1	0.52	0.16	-5.6	-34.1	-20.1	33.8	0.20	<i>bd</i>	-
<b>3g</b> (108934)	11.5	545	125	0.06	103.8	13.5	8.5	10.5	0.78	0.2	-5.8	-32.4	-20.4	29	0.16	<i>bd</i>	-
<b>3h</b> (108935)	11.5	144	27	0.04	19.9	1.7	2.7	0.7	0.12	0.07	-4.8	-31.2	-21.3	88.6	0.17	<i>bd</i>	-
<b>4i</b> (108940)	11.5	243	53	9.02	35.4	3.6	3.21	2.2	0.56	0.11	-5.8	-34	-22.3	64	0.24	<i>bd</i>	-
<b>4j</b> (108941)	11.5	414	89	0.03	80.3	7.1	3.9	11.5	0.64	0.03	-5.7	-34.3	-21.5	49	0.21	<i>bd</i>	-
<b>5k</b> (110737)	42	149	31	0.02	16.9	0.9	2.3	0.7	0.08	0.03	-5.1	-29.4	-22.4	100	0.3	1.24	0.06
<b>5l</b> (80732)	21	200	48	0.1	30	0.33	4.2	0.5	0	0.1	-4.5	-29.7	-24.2	101.5	0.17	1.02	0.03
<b>5m</b> (80735)	21	217	30	0.03	16.5	0.32	10.5	3.6	0	0.11	-4.2	-29.1	-25.3	100.7	0.17	1.47	0.04

1 **Table 2** – Radiocarbon ages of groundwater in the Gellibrand Catchment corrected for calcite  
 2 dissolution. Uncertainties are calculated varying q by  $\pm 0.1$  plus the analytical uncertainty of  $a^{14}\text{C}$   
 3 from *Table 1*

Sample	q	Radiocarbon Age (years)	Uncertainty
1a	0.93	1150	+ 630 / - 980
1b	0.96	1190	+ 360 / - 940
1c	0.93	1520	+ 590 / - 970
2d	0.86	6530	+ 940 / - 1050
2e	0.86	6170	+ 950 / - 1060
3f	0.87	7870	+ 950 / - 1050
3g	0.89	9260	+ 930 / - 1040
3h	0.93	380	+ 630 / - 380
4i	0.97	3440	+ 290 / - 930
4j	0.93	5310	+ 630 / - 980

## 29 **Figure Captions**

30

31 **Figure 1** – Geology, groundwater flow, and cross sectional view of the upper part of the Gellibrand  
32 River Catchment (the Gellibrand Valley). Potentiometric contours for the Eastern View Formation are  
33 created from groundwater data (Water Resources Data Warehouse, 2013) and are expressed in metres  
34 above Australian Height Datum (mAHD). Sampled groundwater bores are also shown. Letters refer to  
35 bores in Table 1.

36 **Figure 2** - (a) Groundwater elevations in bores display clear annual cycles (b) Groundwater head-  
37 gradients in the Gellibrand Valley are upwards implying a discharge zone (Victorian Water Resources  
38 Data Warehouse, 2013) (c) Flow in the Gellibrand River. Baseflow conditions during summer months  
39 transition into high flows in winter following winter rainfall. (Bureau of Meterology, 2013)

40 **Figure 3** – Geochemical characteristics of groundwater in the Eastern View Formation; (a) mCl/Br v  
41 mCl (b) mNa/Cl v mCl (c) mCa v mHCO<sub>3</sub> (d) mSO<sub>4</sub> v mCa. Rainfall samples are also plotted where  
42 measured. Data is from Table 1 with repeat measurements over the sampling period included.

43 **Figure 4** – (a) <sup>2</sup>H vs <sup>18</sup>O values of the Gellibrand River and surrounding groundwater sampled over  
44 March 2011 – August 2013 and the weighted average for rainfall from Adelaide and Melbourne.  
45 MMWL = Melbourne Meteoric Water Line (Hughes and Crawford, 2012). GMWL = Global Meteoric  
46 Water Line (Clarke and Fritz, 1997). Groundwater with <sup>3</sup>H activities > 1 TU are also highlighted.  
47 Data is from Table 1 with repeat measurements over the sampling period included. (b) a<sup>14</sup>C vs <sup>18</sup>O of  
48 groundwater samples.

49 **Figure 5** - (a) Continuous electrical conductivity monitoring of near-river groundwater. **5** (b).  
50 Changes in river height over the study period. Groundwater EC and river level data from deployed  
51 Aqua troll 200 (In-Situ) Data Loggers.

52 **Figure 6** – Historical water table fluctuations 1988-2011 for bore 108927 (Victorian Water Resources  
53 Data Warehouse, 2013). The magnitude of annual recharge cycles are coherent with those recorded in  
54 data loggers over the study period (2011 to 2013)

55 **Figure 7** – Groundwater residences times within the Gellibrand Valley. Residence times up to 9260  
56 years are found in close proximity to the river. Modern local groundwaters with a<sup>14</sup>C > 100 pMC are  
57 situated back on the floodplain. Data from Tables 1 and 2.

58 **Figure 8** – Groundwater flow conceptualisation in the Gellibrand Valley. Though appreciable  
59 amounts of recharge are estimated from bore hydrographs and high river flows, the depth to which  
60 recharging waters infiltrate into the Eastern View Formation (downward leakage) is limited by strong  
61 upward head gradients, and a floodplain which consists of appreciable amounts of silt and clay.

62 **Figure 9** – <sup>14</sup>C age v Cl. <sup>14</sup>C ages are taken from the calcite corrected ages in *Table 1*

63

64

65

66